Multi-dimensional Limiting Strategy for Finite Volume Method and Higher-order Method


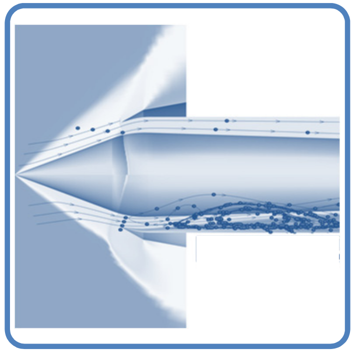
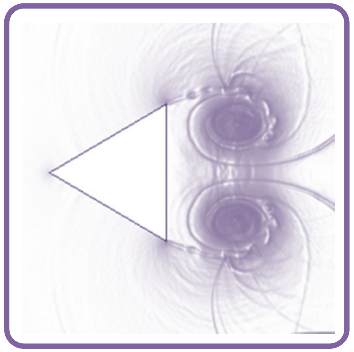

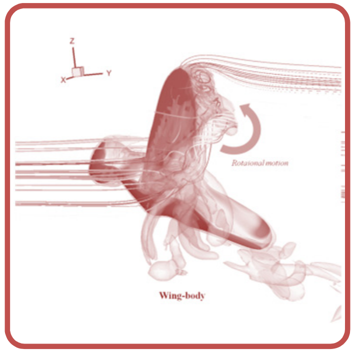

Chongam Kim

Department of Aerospace Engineering

Seoul National University, Korea

11, November, 2013

Limiting Strategy for Higher-Order Methods

- **Higher-order methods**
  - **Accurate capturing of compressive and non-compressive flow features**
  - **Unstructured higher-order methods to handle geometric complexity**
  - **Higher-order methods available**
    - Discontinuous Galerkin (DG) by Cockburn and Shu *et al.*
    - Correction Procedure via Reconstruction (CPR) by Huynh and Wang *et al.*
    - PnPm by Dumbser *et al.*

  →
    - Flexibility to handle complex geometry
    - Compact stencil for higher-order reconstruction
    - Parallelization and *hp*-refinement

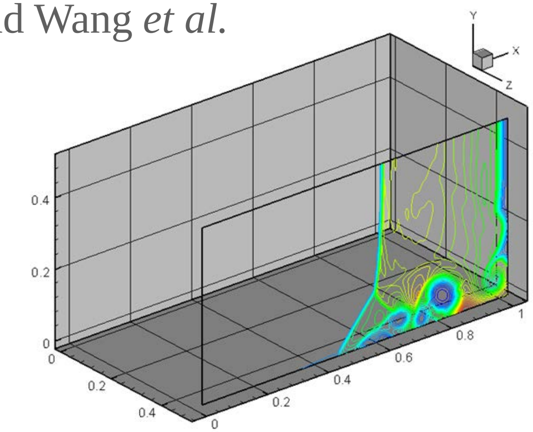

< Shock-boundary interaction >

- **Some issues to be resolved**
  - **Computational cost and memory overhead**
  - **Limiting strategy to control numerical oscillations**

→ Accurate, robust and efficient limiting for higher-order methods

Oscillation Control Strategies in FVM

- **Progresses since 1970s**
  - **Flux Corrected Transport (FCT)**
    - Boris (1973), Zalesak (1984)
  - **MUSCL and Geometric Subcell Reconstruction**
    - Van Leer (1977, 1979)
  - **Total Variation Diminishing (TVD) / Total Variation Bounded (TVB)**
    - Harten (1983), Sweby (1984), Shu (1987)
  - **Essentially Non-Oscillatory (ENO) / Weighted ENO (WENO)**
    - Harten, Shu et al. (1987), Liu et al. (1994)
  - **Spekreijse’s Monotonic Concept**
    - Spekreijse (1989)
  - **Multi-dimensional Reconstruction with Slope Limiter**
    - Barth (1989, 1990)
  - **Local Extremum Diminishing (LED)**
    - A. Jameson (1993)
  - **Adaptive Stencil Reconstruction (ENO/WENO)**
    - Abgrall (1993), Shu (1999)

Limiting Strategy for Multi-dimensional Flows

- **Problems in Multi-dimensional Extension**
  - **Analyses based on one-dimensional flow physics**
    - 1-D SCL of $\dfrac{\partial u}{\partial t}+\dfrac{\partial f(u)}{\partial x}=0$ with $f(u)=au, \dfrac{u^2}{2} \Rightarrow \dfrac{d\bar{u}_j}{dt}=-\dfrac{1}{\Delta x}(\hat{f}_{j+1/2}-\hat{f}_{j-1/2})$
    - Monotonicity constraint on $u_{j+1/2}$: $\min(\bar{u}_j,\bar{u}_{j+1})\le u_{j+1/2}\le \max(\bar{u}_j,\bar{u}_{j+1})$
  - **Multi-dimensional extension by dimensional splitting**
    - 2-D SCL of $\dfrac{\partial u}{\partial t}+\dfrac{\partial f(u)}{\partial x}+\dfrac{\partial g(u)}{\partial y}=0 \Rightarrow \dfrac{d\bar{u}_{i,j}}{dt}=-\dfrac{1}{\Delta x}(\hat{f}_{i+1/2,j}-\hat{f}_{i-1/2,j})-\dfrac{1}{\Delta y}(\hat{g}_{i,j+1/2}-\hat{g}_{i,j-1/2})$
    - Monotonicity constraint by dimensional splitting:

$$\left.\begin{array}{l}(x\text{-}dir)\ \ \min(\bar{u}_{i,j},\bar{u}_{i+1,j})\le u_{i+1/2,j}\le \max(\bar{u}_{i,j},\bar{u}_{i+1,j})\\ (y\text{-}dir)\ \ \min(\bar{u}_{i,j},\bar{u}_{i,j+1})\le u_{i,j+1/2}\le \max(\bar{u}_{i,j},\bar{u}_{i,j+1})\end{array}\right\} \Rightarrow \left\{\begin{array}{l}\text{Is it good enough to handle multi-}\\ \quad\text{dimensional flow situation?}\end{array}\right.$$

  - **Missing flow physics from 1-D to multi-dimensional extension**
    - Treatment of vertex- as well as cell-centered values in limiting is manifested. (Kim *et al*., 2005)
    - For $TV(\bar{u})=\int_V \|\nabla \bar{u}\|_p\, ds$ with $p=1,\ 2,\ \infty,\ \ TV_{two-peaks}<TV_{one-ridge}$ (Jameson, 1995)
    - 2-D TVD scheme is at most first-order accurate. (Goodman and LeVeque, 1985)

Limiting Strategy for Multi-dimensional Flows

- **Interim Summary**
  - **Most oscillation-free schemes have been developed largely based on one dimensional flow physics.**
  - **Dimensional-splitting extension is insufficient or almost impossible to control oscillations in multiple dimensions.**
- **Strategy for Oscillation Control in Multiple Dimensions**
  - **Mimic the nature of multi-dimensional flow physics**
    - MLP limiting condition on both cell-centered and vertex point
  - **Develop an oscillation control stability in multiple dimensions**
    - MLP limiting condition and Discrete Maximum Principle
- **Progress in Multi-dimensional Limiting Strategy**
  - **MLP on structured finite volume method**
    - Kim and Kim (2005), Yoon and Kim (2008)
  - **MLP on unstructured finite volume method**
    - Park and Kim (2010), Park and Kim (2012)
  - **MLP combined with Discontinuous Galerkin (DG) / Correction Procedure via Reconstruction (CPR) method**
    - Park and Kim (2012, 2013)

MLP in Finite Volume Framework

- MLP Condition
- Formulation of MLP on Unstructured Grids
- MLP Limiting and Maximum Principle
- Examples of MLP in FVM

MLP Condition

- **Limiting Condition in Multiple Dimensions:** $\overline{q}_{neighbor}^{\min} \le q \le \overline{q}_{neighbor}^{\max}$
  - Some notation

    : $\vartheta_j =$ the set of all vertices of computational cell T_j

    : $S_{v_i} = \{T_k \mid v_i \in \vartheta_k \text{ for some } i\}$ or

    the union of all computational cells sharing vertex v_i

    : $S_{T_j} = \{T_k \mid v_i \in \vartheta_k \text{ for all } v_i \in \vartheta_j\}$ or

    the union of all computational cells sharing any vertex of T_j (the MLP stencil)

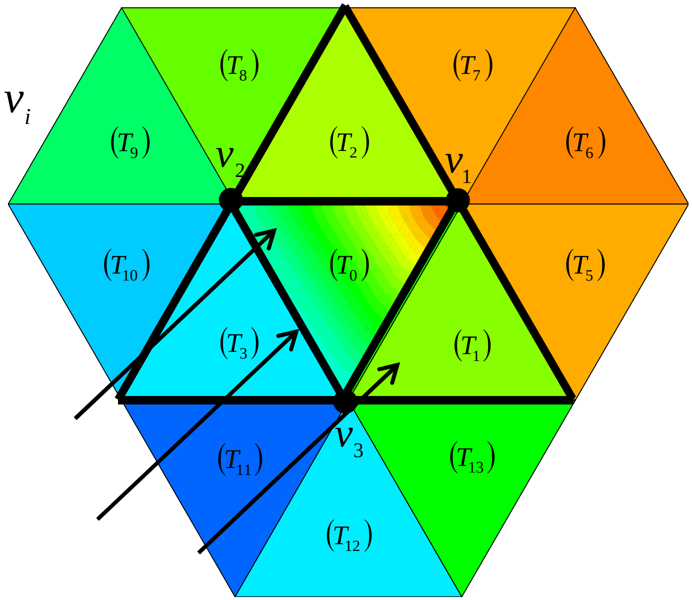

  - With $\overline{q}_{v_i}^{\min} = \min_{T_k \in S_{v_i}}(\overline{q}_k)$ and $\overline{q}_{v_i}^{\max} = \max_{T_k \in S_{v_i}}(\overline{q}_k)$, apply the MLP condition to each vertex point (v_i) of the cell T_0

    $$\overline{q}_{v_i}^{\min} \le q_{v_i} \le \overline{q}_{v_i}^{\max} \quad for\ \forall v_i$$

  - Slope limiting to cell-centered point to satisfy the maximum principle

$\Rightarrow$ Both cell-centered and cell-vertex values satisfy the discrete maximum principle.

MLP Condition (Cont’)

- **Multi-dimensional Limiting Condition on Unstructured Grids**
  - **Constraints on 2-D triangular mesh**

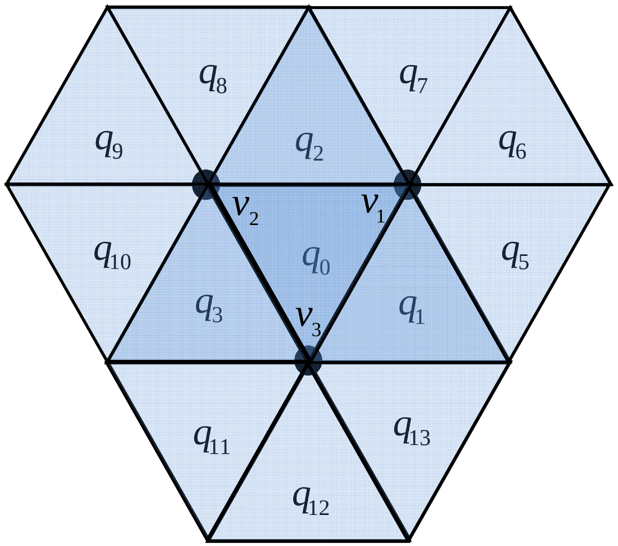

$$\min\begin{pmatrix}\overline{q}_0,\overline{q}_1,\overline{q}_2\\ \overline{q}_5,\overline{q}_6,\overline{q}_7\end{pmatrix}\le q_{v_1}\le\max\begin{pmatrix}\overline{q}_0,\overline{q}_1,\overline{q}_2\\ \overline{q}_5,\overline{q}_6,\overline{q}_7\end{pmatrix},$$

$$\min\begin{pmatrix}\overline{q}_0,\overline{q}_2,\overline{q}_3\\ \overline{q}_8,\overline{q}_9,\overline{q}_{10}\end{pmatrix}\le q_{v_2}\le\max\begin{pmatrix}\overline{q}_0,\overline{q}_2,\overline{q}_3\\ \overline{q}_8,\overline{q}_9,\overline{q}_{10}\end{pmatrix},$$

$$\min\begin{pmatrix}\overline{q}_0,\overline{q}_1,\overline{q}_3\\ \overline{q}_{11},\overline{q}_{12},\overline{q}_{13}\end{pmatrix}\le q_{v_3}\le\max\begin{pmatrix}\overline{q}_0,\overline{q}_1,\overline{q}_3\\ \overline{q}_{11},\overline{q}_{12},\overline{q}_{13}\end{pmatrix}.$$

< 2-D setting >

Formulation of MLP on Unstructured Grids

- **Linear Reconstruction**
  - **Green-Gauss linear reconstruction:** $\nabla\bar{q}_0 = \frac{1}{|T_0|}\int_{\partial T_0} \bar{q}\cdot n dl$
    - Least-square reconstruction

$$\text{with } L_2 \text{ error} = \sum_i \left(\bar{q}_i - \left(\bar{q}_0 + (q_{x,0}\Delta x_{0i} + q_{y,0}\Delta y_{0i} + q_{z,0}\Delta z_{0i})\right)\right)^2$$

$$\begin{bmatrix} \sum \Delta x_{0i}^2 & \sum \Delta x_{0i}\Delta y_{0i} & \sum \Delta z_{0i}\Delta x_{0i} \\ \sum \Delta x_{0i}\Delta y_{0i} & \sum \Delta y_{0i}^2 & \sum \Delta y_{0i}\Delta z_{0i} \\ \sum \Delta z_{0i}\Delta x_{0i} & \sum \Delta y_{0i}\Delta z_{0i} & \sum \Delta z_{0i}^2 \end{bmatrix} \begin{bmatrix} q_{x,0} \\ q_{y,0} \\ q_{z,0} \end{bmatrix} = \begin{bmatrix} \sum \Delta x_{0i}\Delta q_{0i} \\ \sum \Delta y_{0i}\Delta q_{0i} \\ \sum \Delta z_{0i}\Delta q_{0i} \end{bmatrix}$$

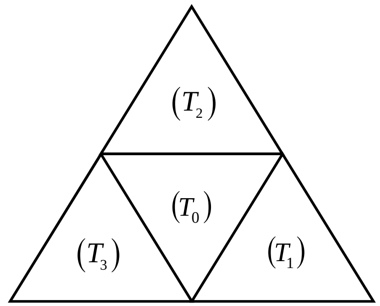

< *Cell-centered control volume* >

- **Slope Limiting using Constraints on vertex v_i**

$$q_0|_{face} = \bar{q}_0 + \phi_{MLP}\nabla\bar{q}_0 \cdot \mathbf{r}_{0,face} \quad \text{with}$$

$$\phi_{MLP} = \min_{\forall v_i \in T_0} \begin{cases} \Phi\left(r_{0,v_i}^{\max}\right) & \text{if } \nabla\bar{q}_0\cdot\mathbf{r}_{0,v_i} > 0 \\ \Phi\left(r_{0,v_i}^{\min}\right) & \text{if } \nabla\bar{q}_0\cdot\mathbf{r}_{0,v_i} < 0, \\ 1 & \text{otherwise} \end{cases}$$

$$\text{where, } r_{0,v_i}^{\max} = \frac{\bar{q}_{v_i}^{\max} - \bar{q}_0}{\nabla\bar{q}_0\cdot\mathbf{r}_{0,v_i}}, \quad r_{0,v_i}^{\min} = \frac{\bar{q}_{v_i}^{\min} - \bar{q}_0}{\nabla\bar{q}_0\cdot\mathbf{r}_{0,v_i}}$$

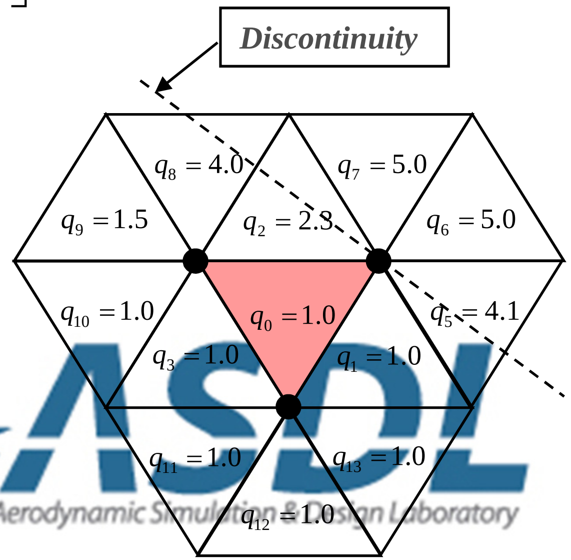

< *2-D setting* >

Formulation of MLP on Unstructured Grids (Cont')

- **Characteristic Limiting Function**
  - **Limiting region to satisfy the maximum principle:** $0 \le \Phi(r) \le \min(1, r)$
  - **Similar to β of MLP on structured meshes, magnitude of slope is adjusted according to the ratio *r*.**
- **MLP-u Limiters (MLP Slope Limiters on Unstructured Grids)**
  - **MLP-u1 limiter**
    - Upper bound of the limiting region: $\Phi(r) = \min(1, r)$
  - **MLP-u2 limiter**
    - Non-differentiable form may degrade convergence of steady-state computations.
    - Adapts the idea of Venkatakrishnan's modification of Barth's limiter (Venkatakrishnan, 1995)
      - ε is to distinguish a nearly smooth region from a fluctuating one.

$$\Phi\left(\frac{\Delta_+}{\Delta_-}\right) = \frac{1}{\Delta_-}\left[\frac{\left(\Delta_+^2 + \varepsilon^2\right)\Delta_- + 2\Delta_-^2\Delta_+}{\Delta_+^2 + 2\Delta_-^2 + \Delta_+\Delta_- + \varepsilon^2}\right] \text{ with } \Delta_+ = \overline{q}_{v_i}^{\max(or\min)} - \overline{q}_0,\ \Delta_- = \nabla \overline{q}_0 \cdot \mathbf{r}_{0,v_i} \text{ and } \varepsilon^2 = \left(K\Delta x\right)^3$$

    - An improved form of ε reflecting the order of spatial error and local flow change

$$\varepsilon^2 = \frac{K_1}{1+r}\Delta\overline{q}_{v_i}^2 \text{ with } r = \frac{\Delta\overline{q}_{v_i}}{K_2\Delta x^{1.5}},\ \Delta\overline{q}_{v_i} = \overline{q}_{v_i}^{\max} - \overline{q}_{v_i}^{\min}, \text{ and } K_1 = K_2 = 5.0$$

      - For nearly constant region, ε becomes large enough to prevent the operation of limiter.
      - For fluctuating region, ε becomes much smaller than local flow variation.

Formulation of MLP on Unstructured Grids (Cont')

- **Implementation of MLP-u Slope Limiting**
  - **Step 1. For the given cell T_j, estimate a local gradient ($\nabla \overline{q}_j$) via a method of linear reconstruction**
    - Least-square or weighted least-square approach
  - **Step 2. For each vertex point v_i of T_j, determine the minimum and maximum cell-averaged values on S_{v_i}**
    - Obtain $\left(\overline{q}_{v_i}^{\min}, \overline{q}_{v_i}^{\max}\right)$ for each vertex in the whole computational domain
  - **Step 3. Determine the allowable local slope on each vertex (r_{j,v_i}) and obtain MLP slope limiter**
    - $\Phi\left(r_{j,v_i}\right)$ is calculated for each vertex and ϕ_{MLP} is taken as the minimum value.
  - **Step 4. For each edge, calculate a numerical flux at edge midpoint**
    - Using the limited linear reconstruction $q_{jk} = \overline{q}_j + \phi_{MLP} \nabla \overline{q}_j \cdot \mathbf{r}_{jk}$, evaluate $h\left(q_{jk}, q_{kj}\right)$

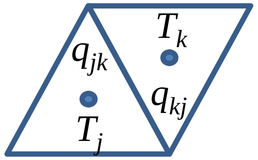

- **Maximum Principle**
  - **Well established in parabolic and elliptic PDE for L_∞ stability**
  - **TVD condition is not available in multi-dimensional situation.**
  - **A primary condition ensuring monotonicity**
    - Cockburn *et al.* (1990), Liu (1993), Barth (2003), Kim *et al.* (2008, 2010, 2012)

MLP Condition and Maximum Principle

- L_∞ **stability of MLP Limiting**
  - ***For a multi-dimensional hyperbolic scalar conservation law of***

$$\frac{\partial q}{\partial t}+\frac{\partial f(q)}{\partial x}+\frac{\partial g(q)}{\partial y}=0,$$

the fully discrete scheme using the MLP limiting satisfies the local maximum principle under a suitable CFL condition.

$$\text{If } \overline{q}_{neighbor}^{\min,n} \le \overline{q}_{i,j}^{n} \le \overline{q}_{neighbor}^{\max,n},\ \text{ then } \ \overline{q}_{neighbor}^{\min,n} \le \overline{q}_{i,j}^{n+1} \le \overline{q}_{neighbor}^{\max,n}.$$

- ($\overline{q}_{neighbor}^{\min,n}, \overline{q}_{neighbor}^{\max,n}$) is determined by the MLP stencil, and the CFL condition is given by

$$\Delta t \frac{L_j}{|T_j|}\left(\sup_{q_1,q_2\in[\overline{q}_{neighbor}^{\min,n},\overline{q}_{neighbor}^{\max,n}]}\left|\frac{\partial h}{\partial q_2}(q_1,q_2)\right|\right)\le\frac{1}{\Gamma} \text{ with } \Gamma_{tri,\ tetra}=3,\ 4 \text{ (Park and Kim, 2010, 2012)}$$

Examples of MLP in FVM

- **Linear Wave**

$$q_t + \mathbf{a} \cdot \nabla q = 0, \ \ \mathbf{a} = (1,2)$$

At t = 1.0

- **Smooth data**

$$q_0(x,y) = \sin(2\pi x)\sin(2\pi y)$$

Scheme	Grid	L_∞	Order	L_1	Order
Barth's Limiter	20x20x2	4.0857E-01	-	1.8795E-01	-
	40x40x2	2.3275E-01	0.81	1.1570E-01	0.70
	80x80x2	1.3716E-01	0.76	6.6048E-02	0.81
	160x160x2	7.7957E-02	0.81	3.6023E-02	0.87
MLP-u1	20x20x2	1.7544E-01		3.3721E-02	
	40x40x2	6.6036E-02	1.41	6.5248E-03	2.37
	80x80x2	2.3412E-02	1.50	1.2439E-03	2.39
	160x160x2	8.0831E-03	1.53	2.5402E-04	2.29
MLP-u2	20x20x2	2.5789E-01		7.0173E-02	
	40x40x2	1.0727E-01	1.27	1.6780E-02	2.06
	80x80x2	4.3619E-02	1.30	4.1919E-03	2.00
	160x160x2	1.7198E-02	1.34	4.1919E-03	2.11
Linear polynomial	20x20x2	3.2729E-02		1.7253E-02	
	40x40x2	6.5138E-03	2.33	3.4741E-03	2.31
	80x80x2	1.4691E-03	2.15	8.0518E-04	2.11
	160x160x2	3.5323E-04	2.06	1.9720E-04	2.03

- **Discontinuous data**

$$q_0(x,y) = \begin{cases} 1 & \text{if } -0.5 \le x, y \le 0. \\ 0 & \text{otherwise} \end{cases}$$

< Contour of solution >

Examples of MLP in FVM (Cont’)

Inviscid Isentropic Vortex

- Initial condition

$$(\rho_\infty, u_\infty, v_\infty, p_\infty) = (1,0,0,1)$$

$$(\delta u, \delta v) = \frac{\beta}{2\pi} e^{(1-r^2)/2}(-\bar{y}, x)$$

$$\delta T = -\frac{(\gamma-1)\beta^2}{8\gamma\pi^2} e^{1-r^2}.$$

- Numerical method
  - RoeM flux scheme
  - 3rd-order TVD-RK
- Grid system: 80x80x2

At $t = 2.0$

Scheme	Grid	L_∞	Order	L_1	Order
Barth’s Limiter	10x10x2	2.0879E-01	-	1.1290E-02	-
	20x20x2	1.1945E-01	0.81	4.7256E-03	1.26
	40x40x2	5.9760E-02	1.00	2.1589E-03	1.13
	80x80x2	3.1982E-02	0.90	1.0712E-03	1.01
MLP-u1	10x10x2	1.7221E-01		9.5917E-03	
	20x20x2	4.1628E-02	2.05	2.5044E-03	1.94
	40x40x2	8.6218E-03	2.27	5.8664E-04	2.09
	80x80x2	1.5848E-03	2.44	1.2895E-04	2.19
MLP-u2	10x10x2	1.8713E-01		1.0430E-02	
	20x20x2	5.7837E-02	1.69	2.8135E-03	1.89
	40x40x2	1.1888E-02	2.28	6.5891E-04	2.09
	80x80x2	2.0363E-03	2.55	1.4320E-04	2.20
Linear polynomial	10x10x2	1.4811E-01		9.7743E-03	
	20x20x2	3.9727E-02	1.9	2.5046E-03	1.96
	40x40x2	7.7253E-03	2.36	5.6202E-04	2.16
	80x80x2	1.5441E-03	2.32	1.2343E-04	2.19

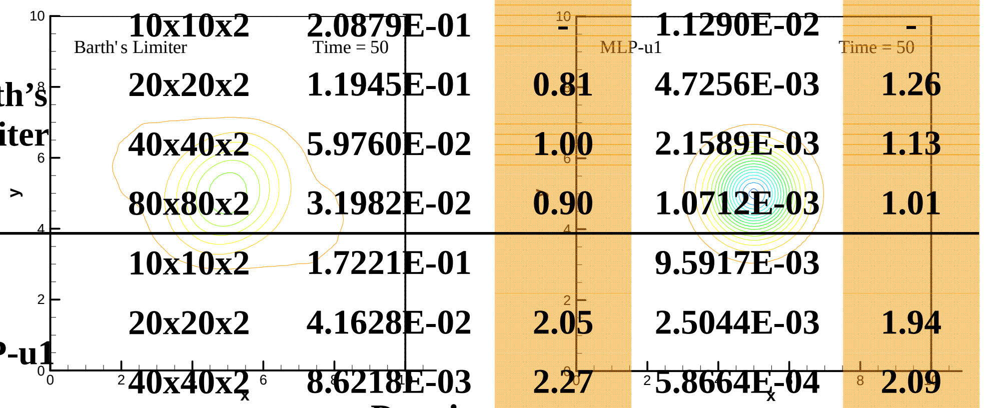

< Density contour >

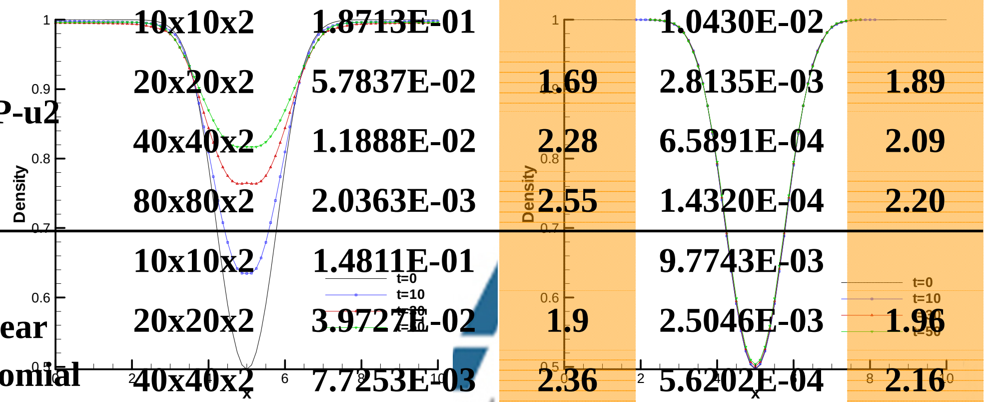

< Density distributions along the center line >

Examples of MLP in FVM (Cont')

- **Transonic Turbulent Flow around RAE2822 Airfoil**

• Numerical method

- Roe's FDS
- LU-SGS method
- Spalart-Allmaras turbulent model

• Free stream: *M=0.729, AOA=2.31, Re = 6.5M*

• Grid system: *Mixed grid (22,842 Cells)*

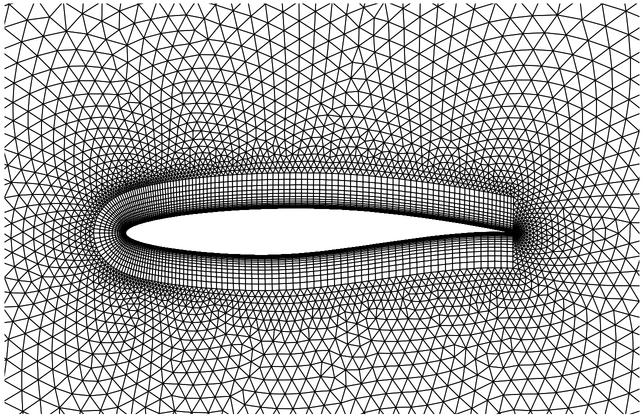

< Grid system >

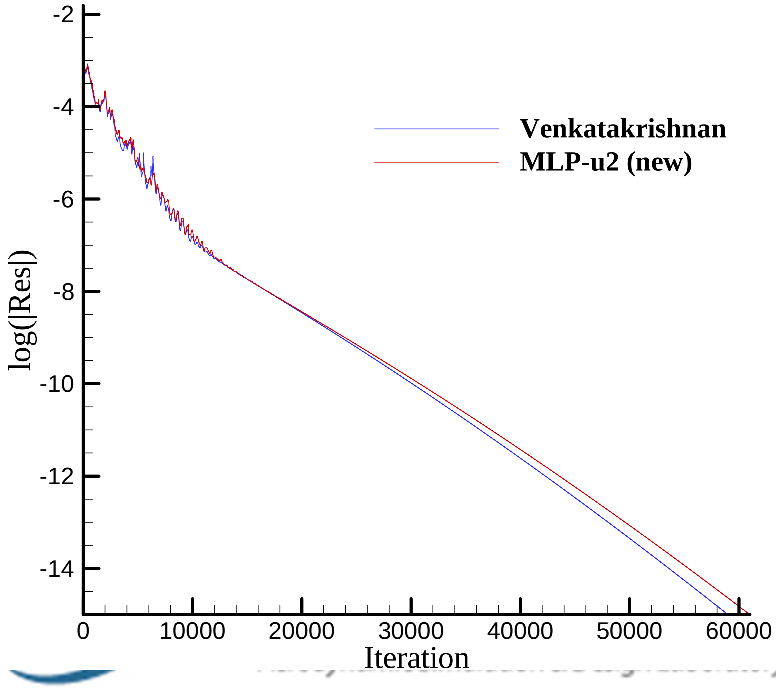

< Error history >

Examples of MLP in FVM (Cont')

Transonic Inviscid Flow around ONERA M6 Wing

- Nu
  - R
  - B
- Fr
  - M
- Gr
  - 3

face >

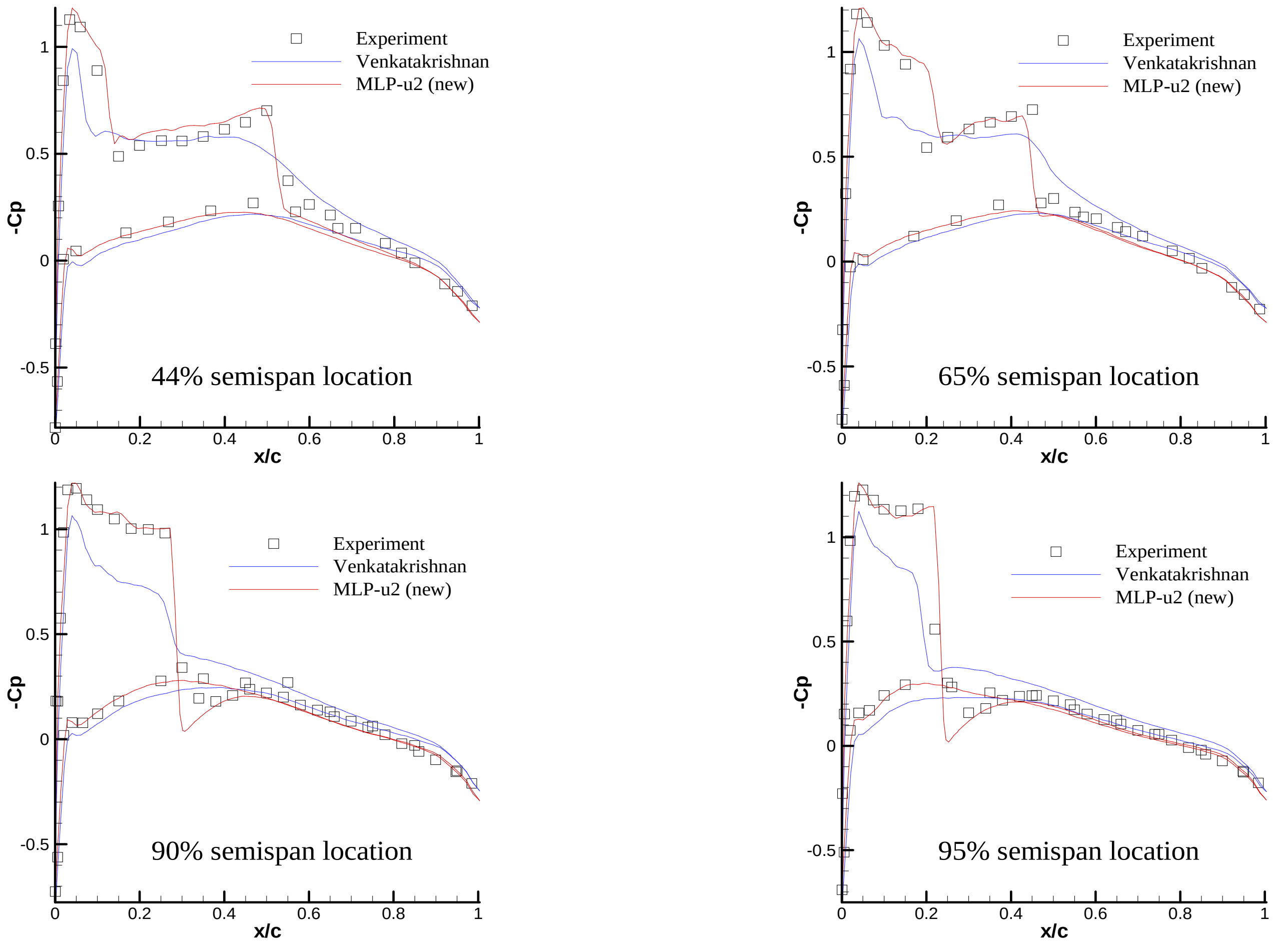

< Pressure coefficients at several wing sections >

Examples of MLP in FVM (Cont')

2-D Viscous Shock Tube Problems

- Numerical method
  - AUSMPW+ flux scheme
  - 3^{rd}-order TVD-RK
- Grid system: *h=1/250, 1/500*

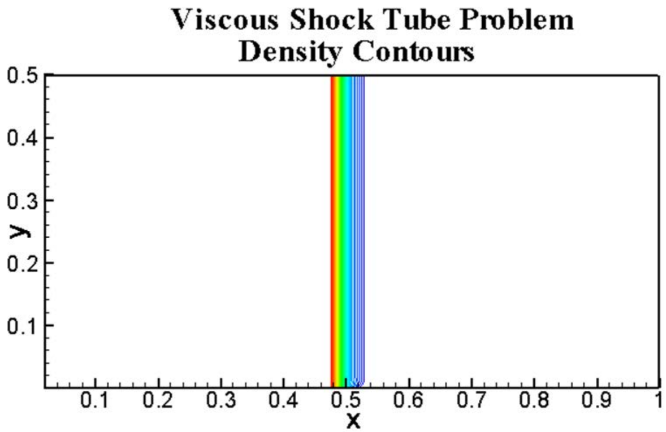

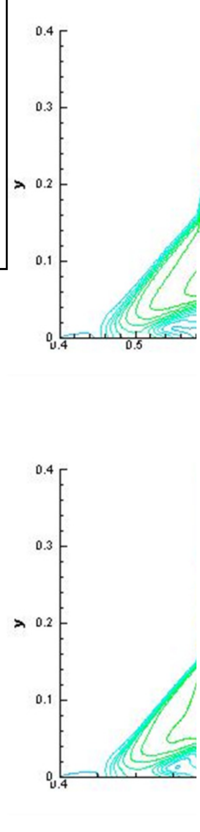

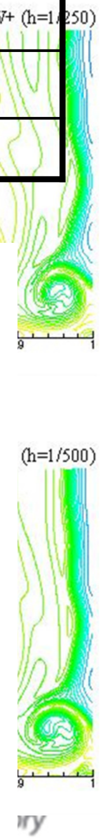

Mesh size	Barth's Limiter	MLP-u1
1/250	0.124	0.147
1/375	0.135	0.161
1/500	0.142	0.168

< Height of the primary vortex >

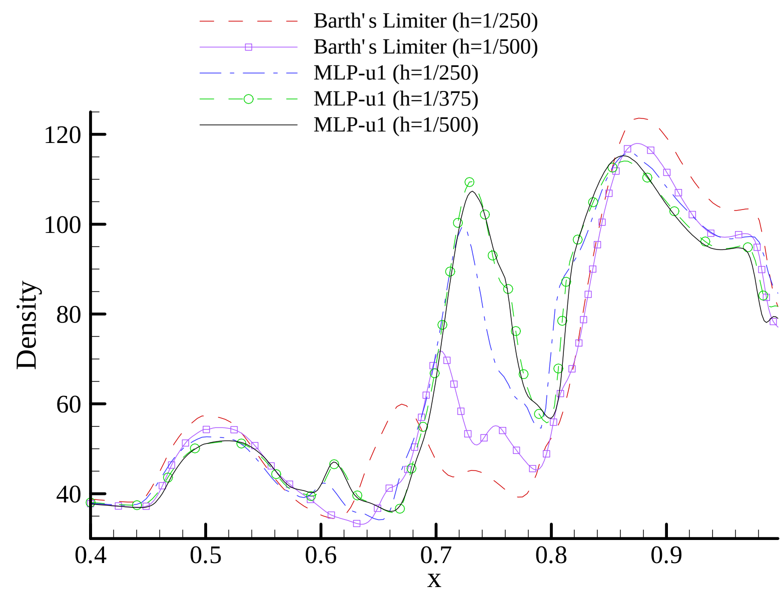

< Density distributions along the bottom wall >

Observations on MLP in FVM

- **Distinctive performance in terms of accuracy and robustness with quite acceptable computational cost**

- **Realization of multi-dimensional monotonicity guided by the MLP condition and the maximum principle**
  - **Local L_∞ stability**

- **Recover the 2nd-order of accuracy with linear reconstruction**

- **Efficient implementation without characteristic decomposition**
  - **All computations are based on conservative variables.**

MLP for Higher-order Methods

- DG Discretization of Conservation Laws
- CPR Discretization of Conservation Laws
- MLP Limiting Strategy for DG and CPR Methods
- Hierarchical MLP for DG and CPR Methods
- Extension to Fluid Systems

- **Discontinuous Galerkin Method for Euler Equations**
  - **Weak form on non-overlapping element T_j**

$$\frac{\partial \mathbf{Q}}{\partial t} + \nabla \cdot \mathbf{F}_c = \mathbf{0} \xrightarrow{\int (\ldots)\phi dV \text{ on } T_j} \int_{T_j} \frac{\partial \mathbf{Q}}{\partial t} \phi dV + \int_{\partial T_j} \mathbf{F}_c \cdot \mathbf{n} \phi dS - \int_{T_j} \mathbf{F}_c \cdot \nabla \phi dV = \mathbf{0}$$

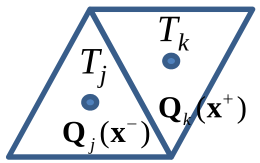

  - **Galerkin approximation on T_j without imposing *C0* continuity**
    - Approximation via shape function: $\mathbf{Q}_j^h(\mathbf{x},t) = \sum_{i=1}^{n} \mathbf{Q}_j^{(i)}(t) b_j^{(i)}(\mathbf{x})$
    - Test function is also approximated with the same space: $\phi = b_j^{(m)}$.
    - $b_j^{(i)}(\mathbf{x})$ is the local orthogonal shape function with $\int_{T_j} b_j^{(m)} b_j^{(n)} = \omega_m \delta_{mn}$.
  - **Convective flux from the conservative numerical flux from FVM**

$$\frac{d}{dt}\int_{T_j} \mathbf{Q}_j^h \mathbf{B}_j dV + \int_{\partial T_j} \mathbf{H}_c\left(\mathbf{Q}_j^h\left(\mathbf{x}^-,t\right), \mathbf{Q}_k^h\left(\mathbf{x}^+,t\right)\right) \cdot \mathbf{n} \mathbf{B}_j dS - \int_{T_j} \mathbf{F}_c\left(\mathbf{Q}_j^h\right) \cdot \nabla \mathbf{B}_j dV = \mathbf{0}$$

    - Boundary and domain integration for *Pn* global accuracy
      - Gauss quadrature rule with *2n* and *2n+1* order of accuracy
- **Diffusion Flux in Navier-Stokes Equations**
  - **BR2 scheme for viscous discretization (Bassi and Rebay et al., 2005)**
    - Primal and auxiliary variable to handle Laplace operator $(\Theta - \nabla \mathbf{Q} = \mathbf{0})$

$$\int_{T_j} \Theta_j^h \mathbf{G}_j dV + \int_{T_j} \mathbf{Q}_j^h \nabla \cdot \mathbf{G}_j dV - \int_{\partial T_j} \mathbf{H}\left(\mathbf{Q}_j^h\left(\mathbf{x}^-,t\right), \mathbf{Q}_k^h\left(\mathbf{x}^+,t\right)\right) \mathbf{G}_j \cdot \mathbf{n} dS = \mathbf{0}$$

DG Discretization of Conservation Laws (Cont')

- **Diffusion Term in Navier-Stokes Equations**
  - **BR2 scheme for viscous discretization (Bassi and Rebay *et al.*, 2005)**
    - Introduce lifting operator to evaluate gradient at a cell-interface in weak sense

$$\int_{T_j} \mathbf{G}_j \left(\Theta_j^h - \nabla \mathbf{Q}_j^h\right) dV = \int_{T_j} \mathbf{G}_j \mathbf{r}_e\left(\left[\mathbf{Q}^h\right]\right) dV = -\int_{\partial T_j} \{\mathbf{G}\}\left[\mathbf{Q}^h\right] dS$$

$$\Theta_j^h = \nabla \mathbf{Q}_j^h + \mathbf{r}\left(\left[\mathbf{Q}^h\right]\right) = \nabla \mathbf{Q}_j^h + \sum_{e \in T_j} \mathbf{r}_e\left(\left[\mathbf{Q}^h\right]\right) \text{ with } \left[\mathbf{Q}^h\right] \equiv \mathbf{Q}^h \mathbf{n}^+ + \mathbf{Q}^h \mathbf{n}^-, \{\mathbf{G}\} = 0.5(\mathbf{G}^+ + \mathbf{G}^-)$$

    - Gradient at the cell-interface

$$\Theta_j^h\left(\mathbf{x}^\pm, t\right) = \nabla \mathbf{Q}_j^h + \mathbf{r}_e\left(\left[\mathbf{Q}^h\right]\right)$$

  - **DG formulation for compressible Navier-Stokes equations**

$$\frac{d}{dt}\int_{T_j} \mathbf{Q}_j^h \mathbf{B}_j dV + \int_{\partial T_j} \mathbf{H}_c\left(\mathbf{Q}_j^h\left(\mathbf{x}^-, t\right), \mathbf{Q}_k^h\left(\mathbf{x}^+, t\right)\right) \cdot \mathbf{n} \mathbf{B}_j dS - \int_{T_j} \mathbf{F}_c\left(\mathbf{Q}_j^h\right) \cdot \nabla \mathbf{B}_j dV$$

$$-\int_{\partial T_j} \mathbf{H}_v\left(\mathbf{Q}_j^h\left(\mathbf{x}^-, t\right), \Theta_j^h\left(\mathbf{x}^-, t\right), \mathbf{Q}_k^h\left(\mathbf{x}^+, t\right), \Theta_k^h\left(\mathbf{x}^+, t\right)\right) \cdot \mathbf{n} \mathbf{B}_j dS + \int_{T_j} \mathbf{F}_v\left(\mathbf{Q}_j^h, \Theta_j^h\right) \cdot \nabla \mathbf{B}_j dV = \mathbf{0}$$

CPR Discretization of Conservation Laws

- **Correction Procedure via Reconstruction (CPR) for Euler Equations**
  - **FR (Huynh, 2007) and LCP (Wang, 2009) are combined and renamed into CPR.**
  - **Strong form on non-overlapping element T_j**

$$\frac{\partial \mathbf{Q}_j^h}{\partial t} + \nabla \cdot \mathbf{F}_c = \mathbf{0} \xrightarrow{\int (\dots)\varphi dV \text{ on } T_j} \int_{T_j} \frac{\partial \mathbf{Q}_j^h}{\partial t} \mathbf{W} dV + \int_{\partial T_j} \left(\mathbf{H}_c - \mathbf{F}_c\right) \cdot \mathbf{n} \mathbf{W} dS + \int_{T_j} \nabla \cdot \mathbf{F}_c \mathbf{W} dV = \mathbf{0}$$

  - **Solution points to represent higher-order reconstruction on each cell**

$$\mathbf{Q}_j^h(\mathbf{x}) = \sum_i \mathbf{Q}_j^{(i)} L_j^{(i)}(\mathbf{x})$$

  - **Lifting operator to approximate the normal flux jump**

$$\int_{T_j} \delta_j \mathbf{W} dV = \int_{\partial T_j} \left(H_c\left(\mathbf{Q}_{jk}^h, \mathbf{Q}_{kj}^h\right) - F_c\left(\mathbf{Q}_{jk}^h\right)\right) \cdot \mathbf{n} \mathbf{W} dS$$

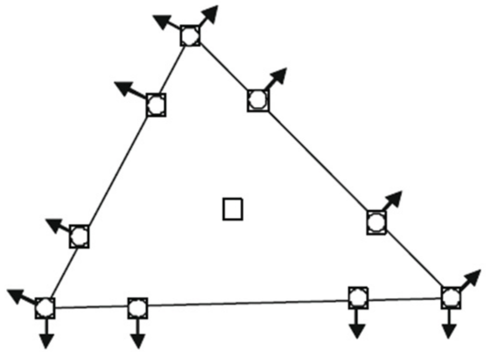

< Solution points (squares) for P3 reconstruction (Wang et al., 2009) >

  - **Project $\nabla \cdot \mathbf{F}\left(\mathbf{Q}_{i,j}^h\right)$ onto polynomial space**

$$\frac{\partial \mathbf{Q}_{i,j}^h}{\partial t} + \prod\left(\nabla \cdot \mathbf{F}\left(\mathbf{Q}_{i,j}^h\right)\right) + \delta_{i,j} = 0$$

    - Approximate $\prod\left(\nabla \cdot \mathbf{F}\left(\mathbf{Q}_{i,j}^h\right)\right) / \delta_{i,j}$ on solution/flux points with Lagrange polynomials
    - Depending on the choice of $\mathbf{W}$, various higher-order methods (DG, SV, SD) can be recovered.

CPR Discretization of Conservation Laws (Cont')

- **Conservation issue**
  - Projection operator for non-linear flux
  - Lagrange polynomial (LP): aliasing error
  - Chain rule violates conservation
  - Conservative CPR (Wang, 2012) to satisfy conservation with additional source term

MLP Limiting Strategy for DG and CPR

- **DG and CPR using Runge-Kutta Method:** $\mathbf{M}\dfrac{d\mathbf{Q}_j^h}{dt} = -\mathbf{R}(\mathbf{Q}^h)$
  - **Runge-Kutta DG Method (RKDG)**
    - One of the frameworks to solve convection-dominated problems (Cockburn and Shu, 2001)
      - Stable time integration: 3-stage 3rd-order TVD-RK and 5-stage 4th-order SSP-RK(5,4)
      - Monotonicity-enforcing limiting procedure
  - **Limiting in DG and CPR**
    - Troubled-cell marker and limiting to the troubled-cells
  - **Troubled-cell marker**
    - Detection of problematic cells requiring a limiting treatment
    - Some methods available
      - TVB marker, KXRCF marker, and so on
    - It may detect some smooth region as a troubled-cell.
  - **Limiting to the troubled-cells**
    - Slope limiting from FVM or WENO-type limiters

⇒

- **Robust and accurate multi-dimensional limiting procedure**
- **Cost-effective limiting without characteristic decomposition**

- **Augmented MLP (A-MLP) Condition for Higher-order Approximation**
  - **For higher-order approximation (greater than *P1*), minimum and maximum value may not occur at vertex.**
  - **A more strict condition to identify the troubled-cells**
  - **Augmented MLP condition**

$$\overline{q}_{v_i}^{\min} \le q_{v_i}^{h,\min} \le q_{v_i}^{h}, \quad q_{v_i}^{h} \le q_{v_i}^{h,\max} \le \overline{q}_{v_i}^{\max}$$

  - **If distributions at any vertex violate the augmented MLP condition, it is tagged as a troubled-cell.**

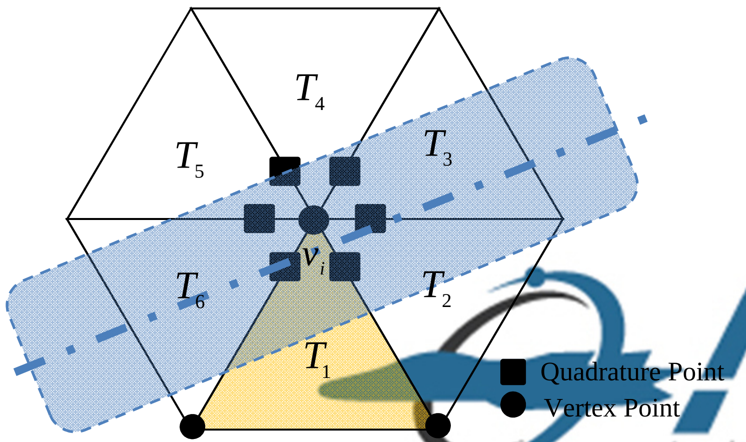

< A-MLP condition to control vertex and quadrature points >

MLP Limiting Strategy for DG and CPR (Cont')

- **Clipping in Slope Limiting**
  - **A simple extrema detector for local smooth extrema:** $\Delta \bar{q}_{v_i} = \bar{q}_{v_i}^{\max} - \bar{q}_{v_i}^{\min} \le K \Delta x^2$
- **MLP Troubled-cell Marker up to *P2* Approximation**
  - **A-MLP condition combined with the simple extrema detector**
  - **Implementation procedure up to *P2* approximation**
    - Step 1. Compute the MLP-based troubled-cell maker D_{v_i} for *Pn* $(n \le 2)$ approximation at every vertex v_i of the cell T_j

$$D_{v_i} = \begin{cases} 1 & \text{if A-MLP condition or simple extrema detector is satisfied.} \\ 0 & \text{otherwise} \end{cases}$$

    - Step 2. A troubled-cell is detected if $\min\limits_{v_i \in T_j}\left(D_{v_i}\right) = 0.$
    - Step 3. For the troubled-cell,
      - If $n=2$, project the *P2* approximation into the linear space V^1 ($q_j^{h,P1}(\mathbf{x}) = \Pi^1 q_j^{h,P2}(\mathbf{x})$), and go to Step 1
      - If $n=1$, apply the MLP-u slope limiter developed in FVM

$$\tilde{q}_j^{h,P1}(\mathbf{x},t) = \bar{q}_j + \phi_{MLP}\left(q_j^{h,P1} - \bar{q}_j\right)$$

    For the normal cell, *Pn* approximation is preserved.

Hierarchical MLP for DG and CPR

- **MLP Limiting for Arbitrary Order of Accuracy ($Pn,\ n \geq 2$)**
  - **Optimal choice of K for smooth extrema detector may depends on n if $n \geq 2$.**

    → ***K* is eliminated by examining the behavior of local smooth extrema at vertex v_i.**
    - Split $q_j^{h,Pn}(\mathbf{x}_{v_i})$ into cell-averaged, linear and higher-order parts

      $$q_j^{h,Pn}\left(\mathbf{x}_{v_i}\right) = \overline{q}_j + \underbrace{\left(L\left(\mathbf{x}_{v_i}\right) - \overline{q}_j\right)}_{Pn-\text{projected slope}} + \underbrace{\left(q_j^{h,Pn}\left(\mathbf{x}_{v_i}\right) - L\left(\mathbf{x}_{v_i}\right)\right)}_{P1-\text{filtered } Pn} \quad \text{with}$$

      $$L(\mathbf{x}) = \Pi^1 q_j^{h,Pn}(\mathbf{x}) : \text{projection of } q_j^{h,Pn}(\mathbf{x}) \text{ onto } P1 \text{ space}$$

      • C1. if local maximum near v_i, Pn-projected slope > 0, $P1$-filtered $Pn < 0$, $q_j^{h,Pn}\left(\mathbf{x}_{v_i}\right) > \overline{q}_{v_i}^{\min}$

      • C2. if local minimum near v_i, Pn-projected slope < 0, $P1$-filtered $Pn > 0$, $q_j^{h,Pn}\left(\mathbf{x}_{v_i}\right) < \overline{q}_{v_i}^{\max}$
    - Deactivation threshold to avoid nearly constant region

      $$\left| q_j^{h,Pn}\left(\mathbf{x}_{v_i}\right) - \overline{q}_j \right| \leq \max\left(\varepsilon \left|\overline{q}_j\right|, \left|T_j\right|\right)$$

      - Small number ($\varepsilon = 1 \times 10^{-3}$) to distinguish a constant region with machine error
  - **Hierarchical MLP limiting from (C1, C2) and A-MLP conditions**

    $$q_j^{h,P2}(\mathbf{x}) = \overline{q}_j + \phi_{MLP}\left(P1_j(\mathbf{x})\right) + \varphi_j^{P2}\left(P2_j(\mathbf{x})\right),$$

    $$q_j^{h,P3}(\mathbf{x}) = \overline{q}_j + \phi_{MLP}\left(P1_j(\mathbf{x})\right) + \varphi_j^{P2}\left(P2_j(\mathbf{x}) + \varphi_j^{P3}\left(P3_j(\mathbf{x})\right)\right),$$

    ...

    $$q_j^{h,Pn}(\mathbf{x}) = \overline{q}_j + \phi_{MLP}\left(P1_j(\mathbf{x})\right) + \varphi_j^{P2}\left(P2_j(\mathbf{x}) + \varphi_j^{P3}\left(P3_j(\mathbf{x}) + \varphi_j^{P4}\left(\ldots + \varphi_j^{Pn} Pn_j(\mathbf{x})\right)\right)\right).$$

Hierarchical MLP for DG and CPR (Cont')

- **Hierarchical MLP limiting from (C1, C2) and A-MLP conditions**
  - Limiting is applied hierarchically to each *Pm* mode.
    - $q_j^{h,Pn}(\mathbf{x}) = \bar{q}_j + \phi_{MLP}\left(P1_j(\mathbf{x})\right) + \varphi_j^{P2}\left(P2_j(\mathbf{x}) + \varphi_j^{P3}\left(P3_j(\mathbf{x}) + \varphi_j^{P4}\left(\ldots + \varphi_j^{Pn} Pn_j(\mathbf{x})\right)\right)\right)$

    with $Pm_j(\mathbf{x}) = \Pi^m q_j^{h,Pn}(\mathbf{x}) - \Pi^{m-1} q_j^{h,Pn}(\mathbf{x})$, $\Pi^m q_j^{h,Pn}(\mathbf{x})$: projection of $q_j^{h,Pn}(\mathbf{x})$ onto *Pm* space
  - Hierarchical troubled-cell marker: $\varphi_j^{Pn} = \min_{\forall v_i \in T_j}\left(\psi_{v_i,j}^{Pn}\right)$

$$\psi_{v_i,j}^{Pn} = \begin{cases} 1 & \text{if (C1, C2) with clipping or A-MLP condition is satisfied.} \\ 0 & \text{otherelse} \end{cases}$$

- **Implementation of Hierarchical MLP Limiting for *Pn* with $n \geq 2$**
  - Step 1. Check A-MLP condition with *Pn* approximation at each vertex v_i of the cell T_j
  - Step 2. Check (C1, C2) conditions, and compute the hierarchical troubled-cell marker φ_j^{Pn}
  - Step 3. If tagged as a normal cell $(\varphi_j^{Pn} = 1)$, *Pn* approximation is kept unlimited. Otherwise, if $n > 2$, project it onto V^{n-1} space, obtain $P(n-1)_j(x)$ and go to Step 1

$$P(n-1)_j(\mathbf{x}) = \Pi^{n-1} q_j^{h,Pn}(\mathbf{x}) - \Pi^{n-2} q_j^{h,Pn}(\mathbf{x})$$

  if $n = 2$, project it onto V^1 space and apply the MLP-u slope limiter from FVM

$$\tilde{q}_j^{h,P1}(\mathbf{x},t) = \bar{q}_j + \phi_{MLP}\left(q_j^{h,P1} - \bar{q}_j\right)$$

- **Projection operator in DG and CPR** $(\Pi^m q_j^{h,Pn}(\mathbf{x}))$
  - DG: For $q_j^{h,Pn}(\mathbf{x}) = \sum_{i=1}^{n} q_j^{(i)} b_j^{(i)}(\mathbf{x})$, $\Pi^m q_j^{h,Pn}(\mathbf{x}) = \sum_{i=1}^{m} q_j^{(i)} b_j^{(i)}(\mathbf{x})$ by discarding all $q_j^{(i)}$ greater than m
  - CPR: For $q_j^{h,Pn}(\mathbf{x}) = \sum_{i=1}^{n} q_j^{(i)} L_j^{(i)}(\mathbf{x})$, $\sum_{i=1}^{m} \tilde{q}_j^{(i)} \tilde{L}_j^{(i)}(\mathbf{x})$ by $L2$ projection $\xrightarrow[\text{of } q_j^{h,Pn}(\mathbf{x})]{\tilde{q}_j^{(i)} \text{ for solution points}}$ $\Pi^m q_j^{h,Pn}(\mathbf{x}) = \sum_{i=1}^{n} \tilde{\tilde{q}}_j^{(i)} L_j^{(i)}(\mathbf{x})$

Hierarchical MLP for DG and CPR (Cont')

- **Hierarchical MLP Limiting for *Pn* with *n*≥2**

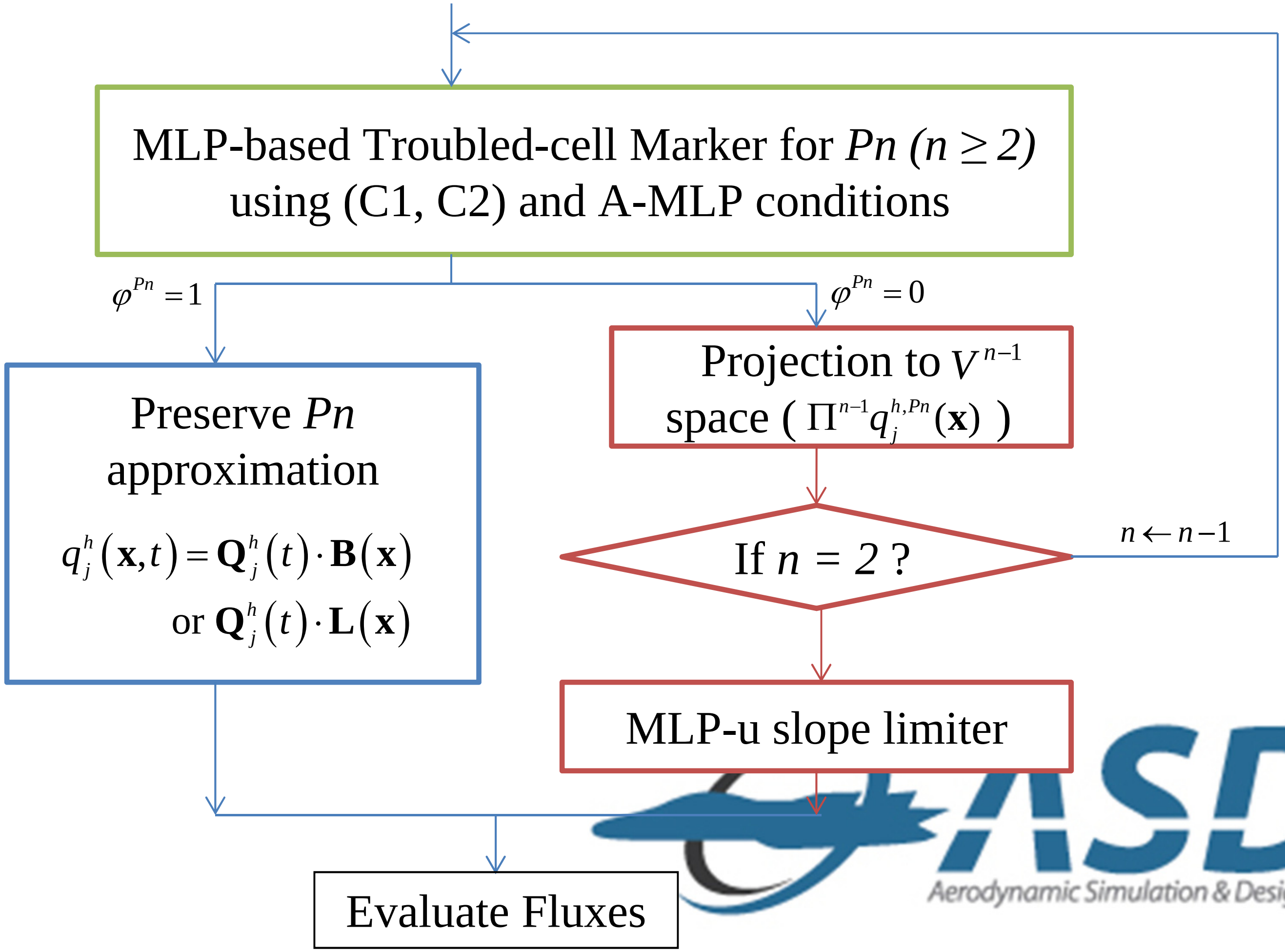

Hierarchical MLP for DG and CPR (Cont')

- **Validation of Extrema Detection with 2-D Profiles**
  - **2-D Gaussian hump (1/4), Spike (2/4), Half ellipse (3/4) and Square (4/4)**

$$q_0 = \begin{cases} G(r_1,\beta,-\delta)+G(r_1,\beta,0)+G(r_1,\beta,\delta) & 0.1<x<0.3,\ 0.1<y<0.3 \\ \max(1-10r_2,0) & -0.3<x<-0.1,\ 0.1<y<0.3 \\ \left(F(r_3,\alpha,-\delta)+4F(r_3,\alpha,0)+F(r_3,\alpha,\delta)\right)/6 & -0.3<x<-0.1,\ -0.3<y<-0.1, \\ 1 & 0.1<x<0.3,\ -0.3<y<-0.1 \\ 0 & else \end{cases}$$

$$G(x,\beta,x_c)=\exp\left(-\beta(x-x_c)^2\right)$$

$$F(x,\alpha,x_c)=\sqrt{\max\left(1-\alpha^2(x-x_c)^2,0\right)}$$

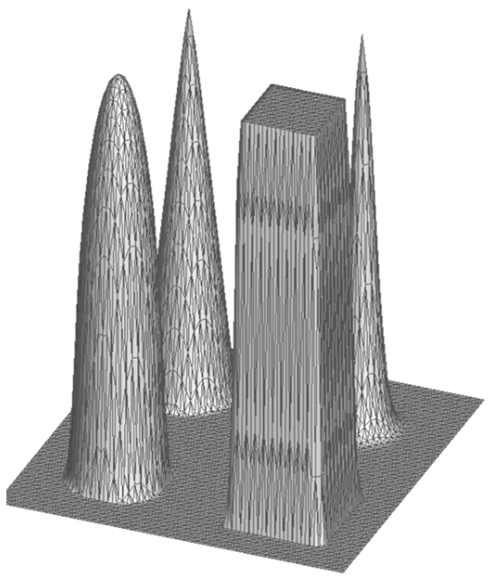

< *3-D shape* >

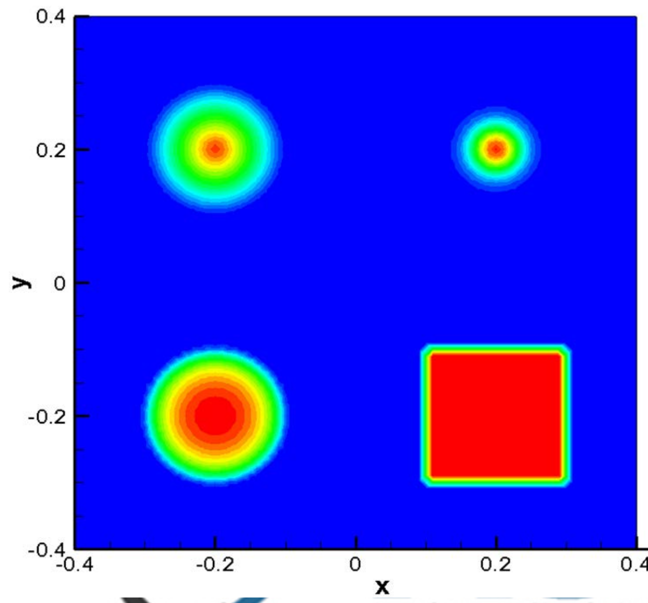

< *Contour of initial profile* >

Hierarchical MLP for DG and CPR (Cont')

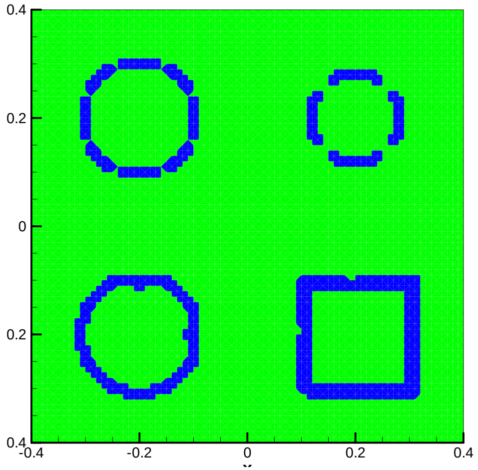

< Simple detector, DG-P1, K = 100 >

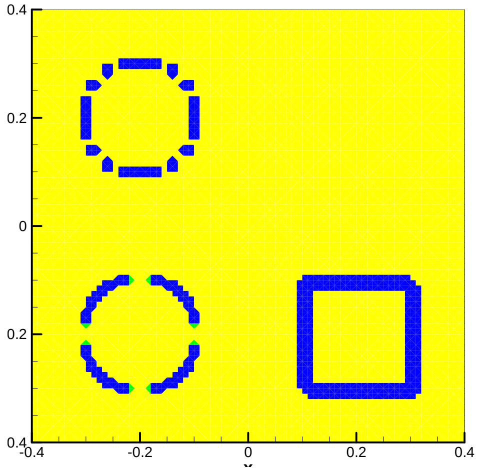

< Simple detector, DG-P2, K = 100 >

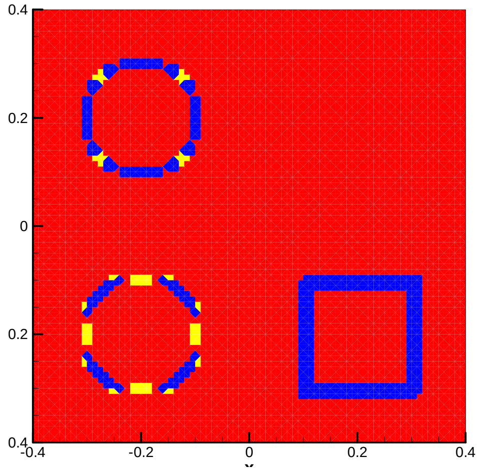

< Simple detector, DG-P3, K = 100 >

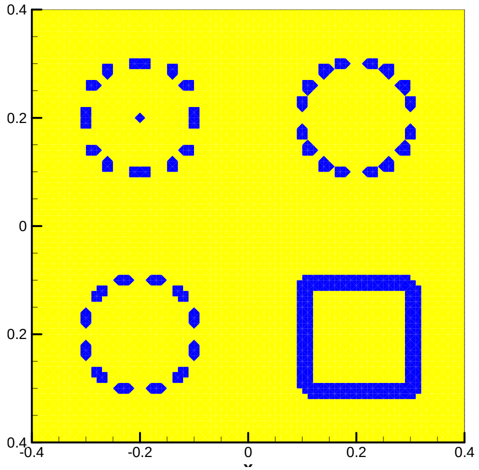

< Hierarchical detector, DG-P2 >

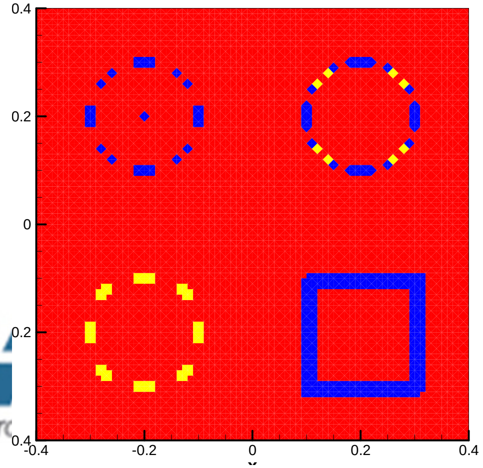

< Hierarchical detector, DG-P3 >

Hierarchical MLP for DG and CPR (Cont')

- **Linear Wave**

  $$q_t + \mathbf{a}\cdot\nabla q = 0,\ \ \mathbf{a} = (1,2)$$

  - **Discontinuous data**

    $$q_0 = \begin{cases} 1 & \text{if} \quad 0.25 \le x, y \le 0.75 \\ 0 & \text{otherwise} \end{cases}$$

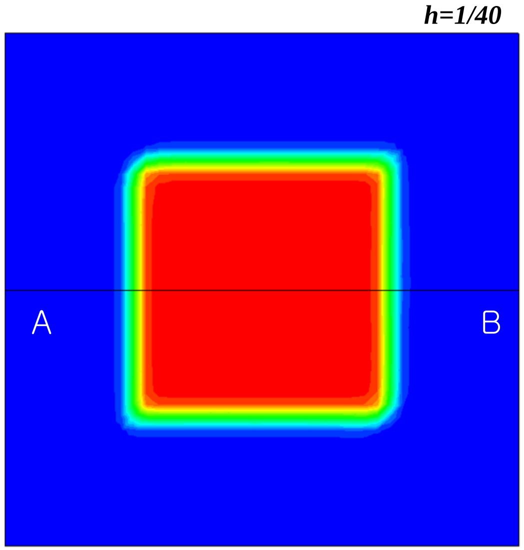

< Numerical solution at t = 1 >

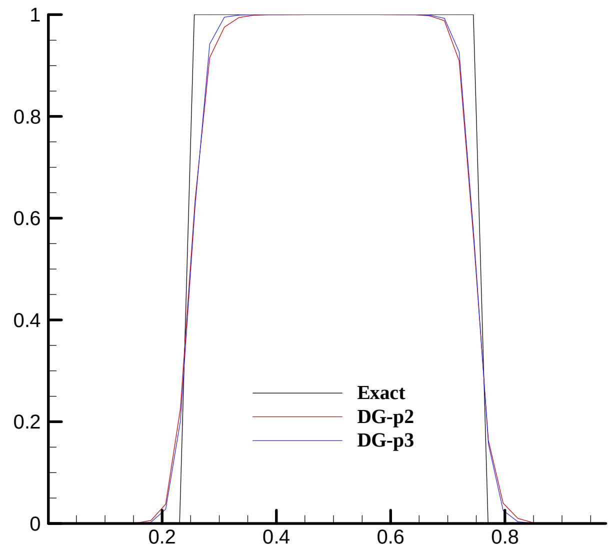

< Distribution along line AB >

Hierarchical MLP for DG and CPR (Cont')

- **2-D Convection-Diffusion Equation**
  - **Linear scalar equation**

$$q_t + q_x + q_y = \frac{2a}{\pi^2} q_{xx} + \frac{2a}{\pi^2} q_{yy}, \quad a = 0.02$$

$$q_0(x, y) = \sin\left(0.5\pi(x + y)\right)$$

  - **Computational domain : [-2, 2]x[-2, 2] with periodic boundary condition**

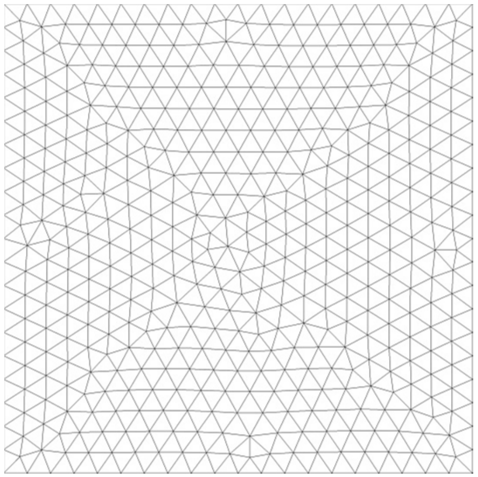

< Coarse grid >

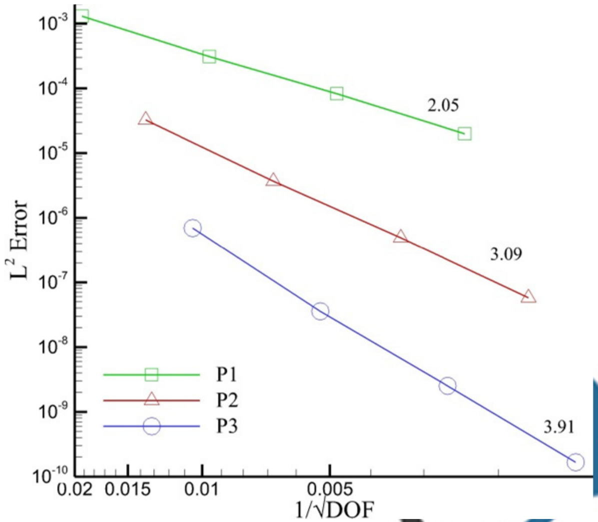

< L_2 Error >

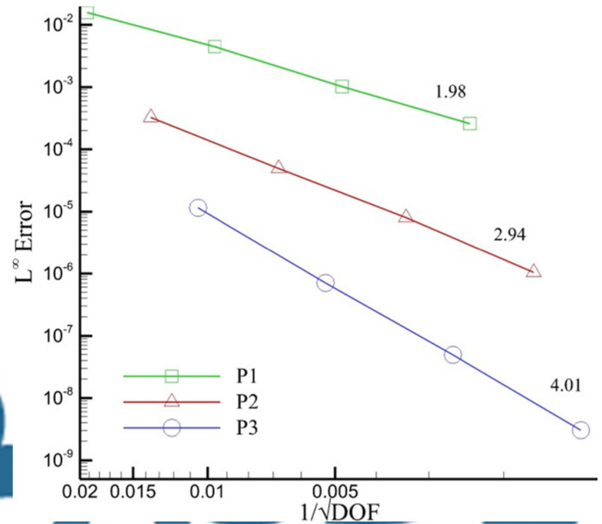

< L_∞ Error >

Hierarchical MLP for DG and CPR (Cont')

- **2-D Burgers Equation**

$$q_t + \left(\frac{q^2}{2}\right)_x + \left(\frac{q^2}{2}\right)_y = 0,\ \ q_0 = \frac{1}{2} + \sin\left(\frac{\pi(x+y)}{2}\right)$$

  - **Formation of shock (*t = 0.5*)**

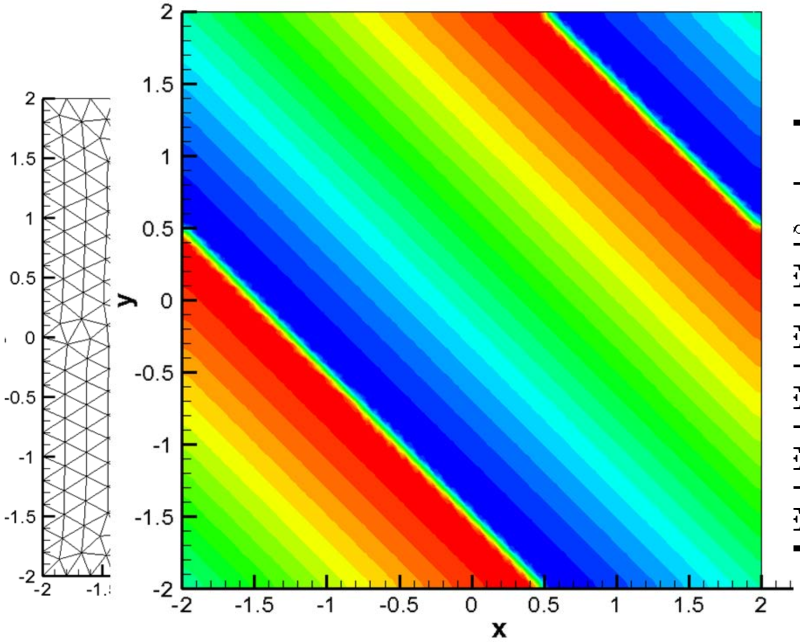

< Contour of DG-P3 at t = 0.5 >

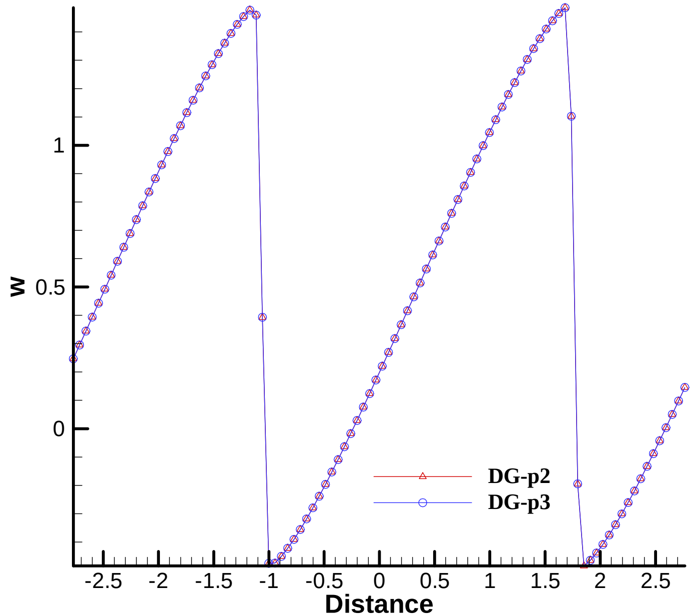

< Distribution along a diagonal at t = 0.5 >

Hierarchical MLP for DG and CPR (Cont')

- **3-D Burgers Equation with a Smooth Profile**

$$q_t + \left(\frac{q^2}{2}\right)_x + \left(\frac{q^2}{2}\right)_y + \left(\frac{q^2}{2}\right)_z = 0, \quad q_0 = 0.3 + 0.7\sin\left(\frac{x+y+z}{3}\right)$$

  - **Computed results ($t = 0.05$)**

	DG-P2, MLP-u1				DG-P3, MLP-u1			
	L_∞		L_1		L_∞		L_1	
8x8x8x6	1.9700E-03		5.9128E-04		2.0151E-04		6.1977E-05	
12x12x12x6	6.7837E-04	2.63	2.1015E-04	2.55	4.1630E-05	3.89	1.3568E-05	3.75
16x16x16x6	3.0360E-04	2.79	9.6650E-05	2.70	1.3438E-05	3.93	4.0190E-06	4.23
24x24x24x6	1.0724E-04	2.57	2.8870E-05	2.98	3.0607E-06	3.65	8.6874E-07	3.78
32x32x32x6	4.9034E-05	2.72	1.1961E-05	3.06	1.0491E-06	3.72	3.0028E-07	3.69
48x48x48x6	1.4902E-05	2.93	3.5831E-06	2.97	1.9123E-07	4.20	4.6375E-08	4.61

- **TC Marker and Limiting for Euler / Navier-Stokes Equations**
  - **Density (or entropy) variation can be used as an indicator to capture physical discontinuity.**
  - **MLP limiting to conservative variables**
- **Convergence Study for Inviscid Flow**
  - **Isentropic vortex advection with initial mean flow and perturbation given by**

$$(\delta u, \delta v) = \frac{\varepsilon}{2\pi} e^{0.5(1-r^2)} (-\bar{y}, \bar{x}),\ \delta T = -\frac{(\gamma - 1)\varepsilon^2}{8\gamma\pi^2} e^{1-r^2},\ \delta S = 0,\ (u, v) = (1,1) \text{ at } t = 10.0$$

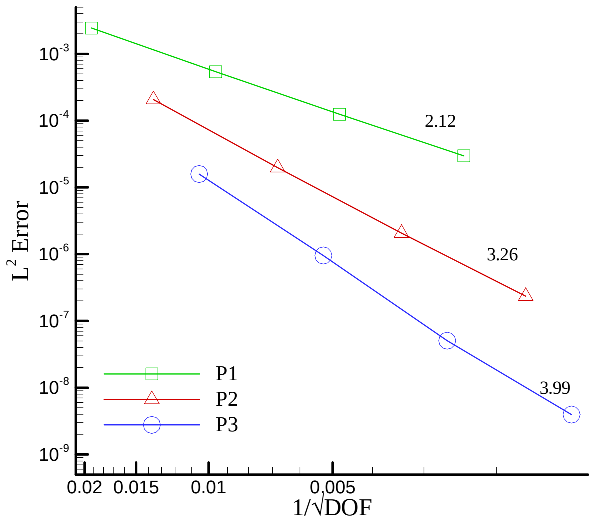

< L_2 error >

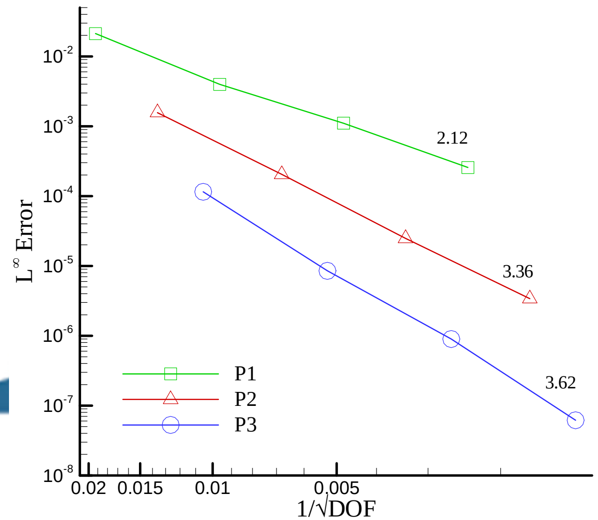

< L_∞ error >

Extension to Fluid Systems (Cont')

- **Convergence Test for Viscous Flow**
  - **Navier-Stokes equations**

$$\mathbf{Q}_t + \nabla \cdot \left(\mathbf{F}_c - \mathbf{F}_v \right) = \mathbf{S}, \quad \mathrm{Re} = 2000, \quad \mathrm{Pr} = 0.72$$

$$\rho = e = \sin\left(\mathbf{k} \cdot \mathbf{x} - \omega t \right) + c, \ (u, v) = (1,1)$$

  - **Computational domain: [0, 2]x[0, 2] with periodic boundary condition**

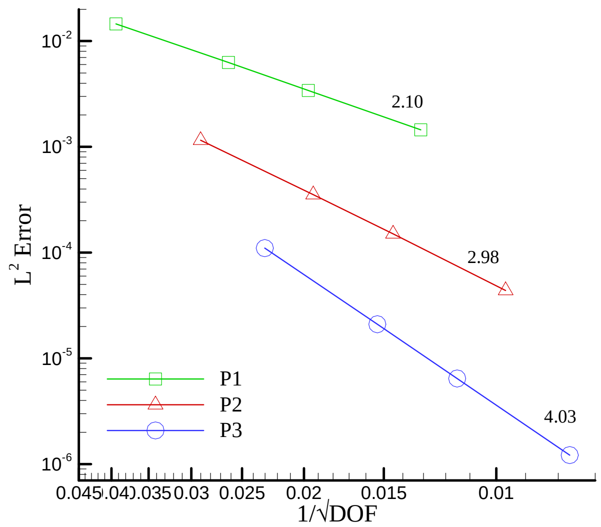

$< L_2$ ***error*** $>$

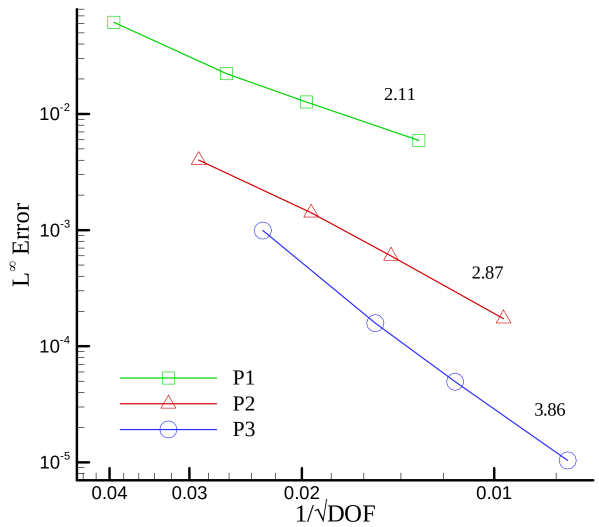

$< L_\infty$ ***error*** $>$

Numerical Results

- Double Mach Reflection
- A Mach 3 Wind Tunnel with a Step
- Shock Interaction with Wedge
- Interaction of Shock Wave with Density Bubble
- Viscous Shock-Vortex Interactions
- Oblique Shock-Mixing Layer Interactions

- **Double Mach Reflection with a Strong Shock**
  - **Standard test case for high resolution schemes**
  - **Numerical scheme**
    - **Numerical flux: AUSMPW+ scheme**
  - **Computational domain**

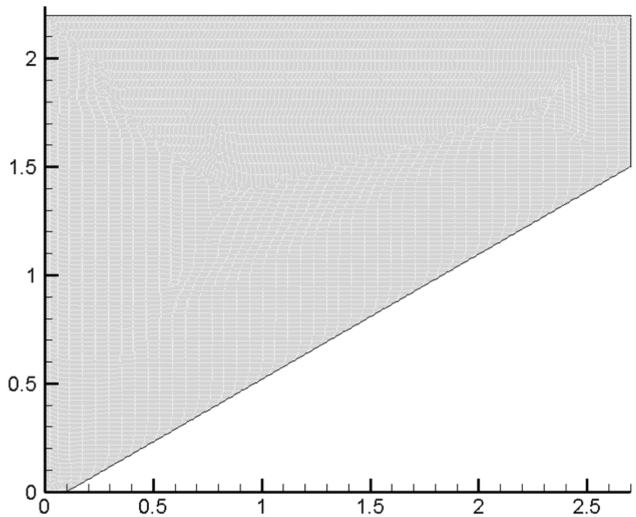

  - **Computational cost**

	DG-P2	DG-P3	CPR-P2	CPR-P3
Work Unit	1	2.26	0.81	2.02

Double Mach Reflection (Cont')

- **Flow physics around the Mach stem**

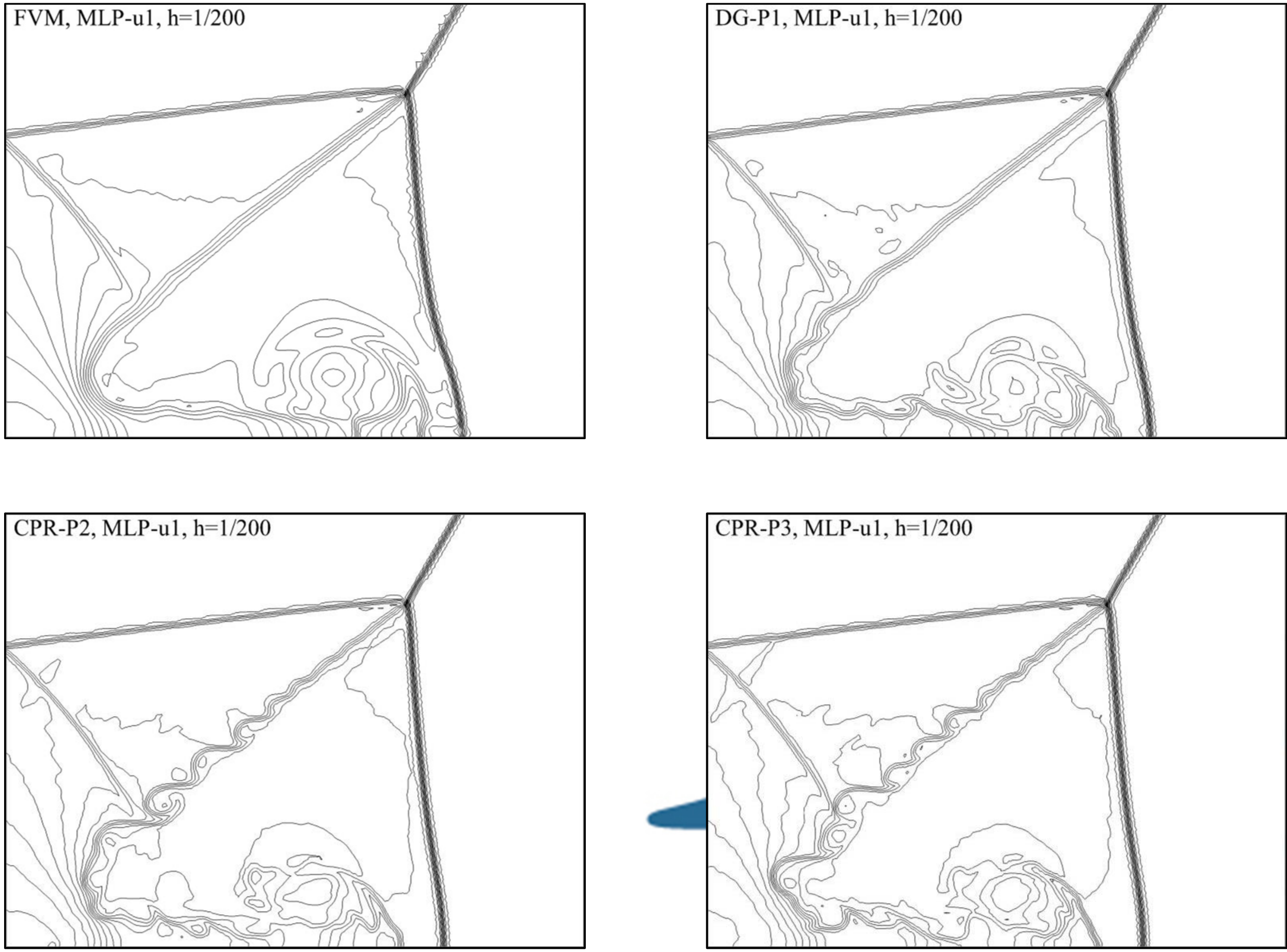

Double Mach Reflection (Cont')

- **Comparison with other limiters**

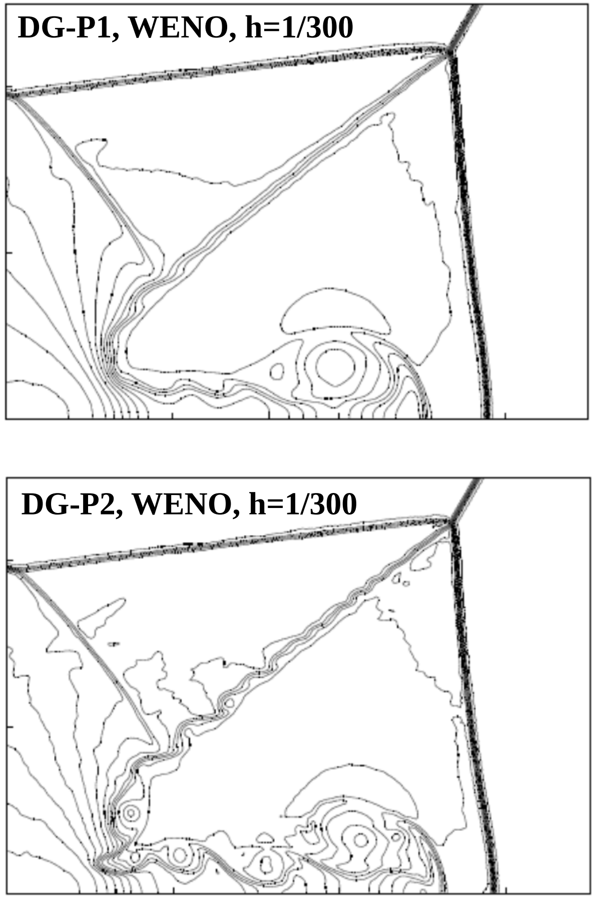

< DG with WENO limiter, TVB Marker, Zhu et al., 2008 >

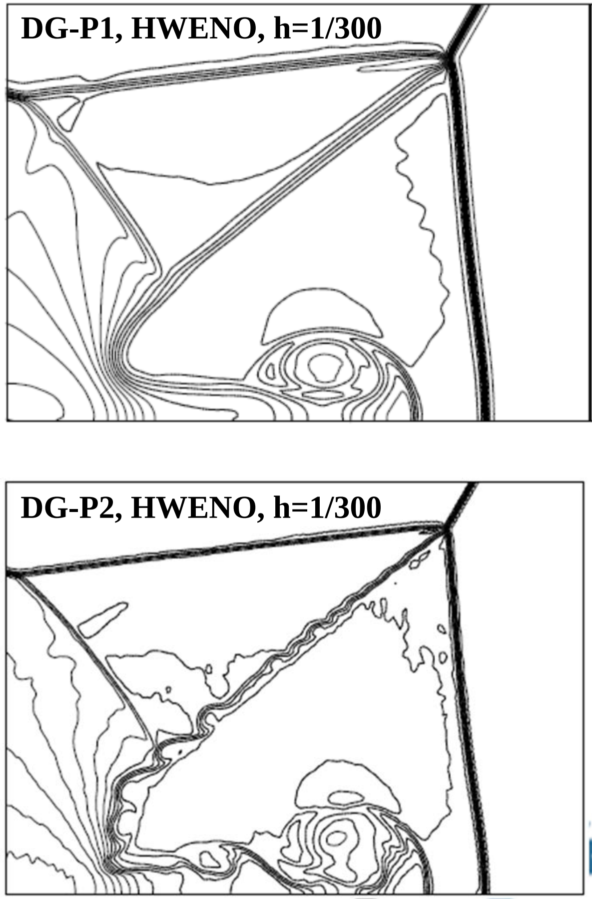

< DG with HWENO limiter, KXRCF Marker, Zhu & Qiu., 2009 >

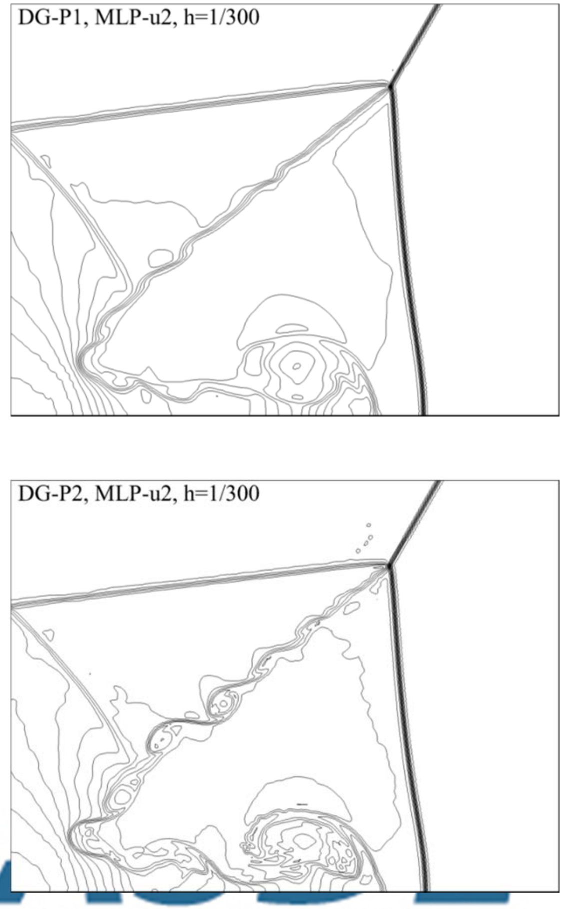

< DG-MLP >

- **A Mach 3 Wind Tunnel with a Step**
  - **Standard test case for high resolution schemes**
  - **Numerical scheme**
    - **Numerical flux: RoeM**
    - **MLP-u slope limiters**
  - **Singularity point is treated by refining the mesh near the corner.**

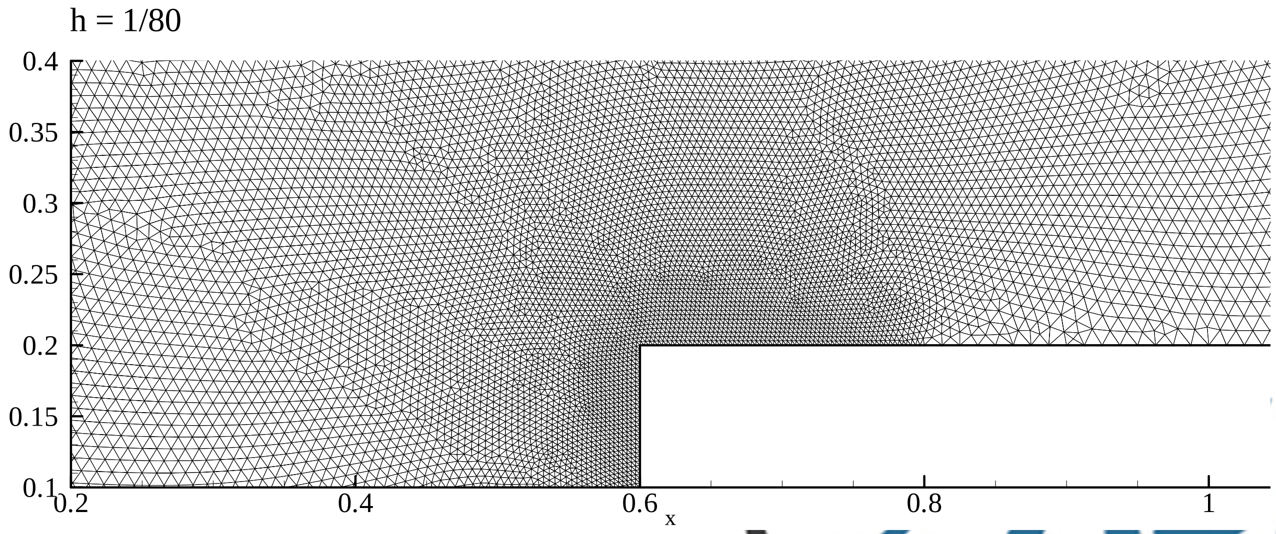

< Grid near the corner >

A Mach 3 Wind Tunnel with a Step (Cont')

- **Resolution of the shear layer**

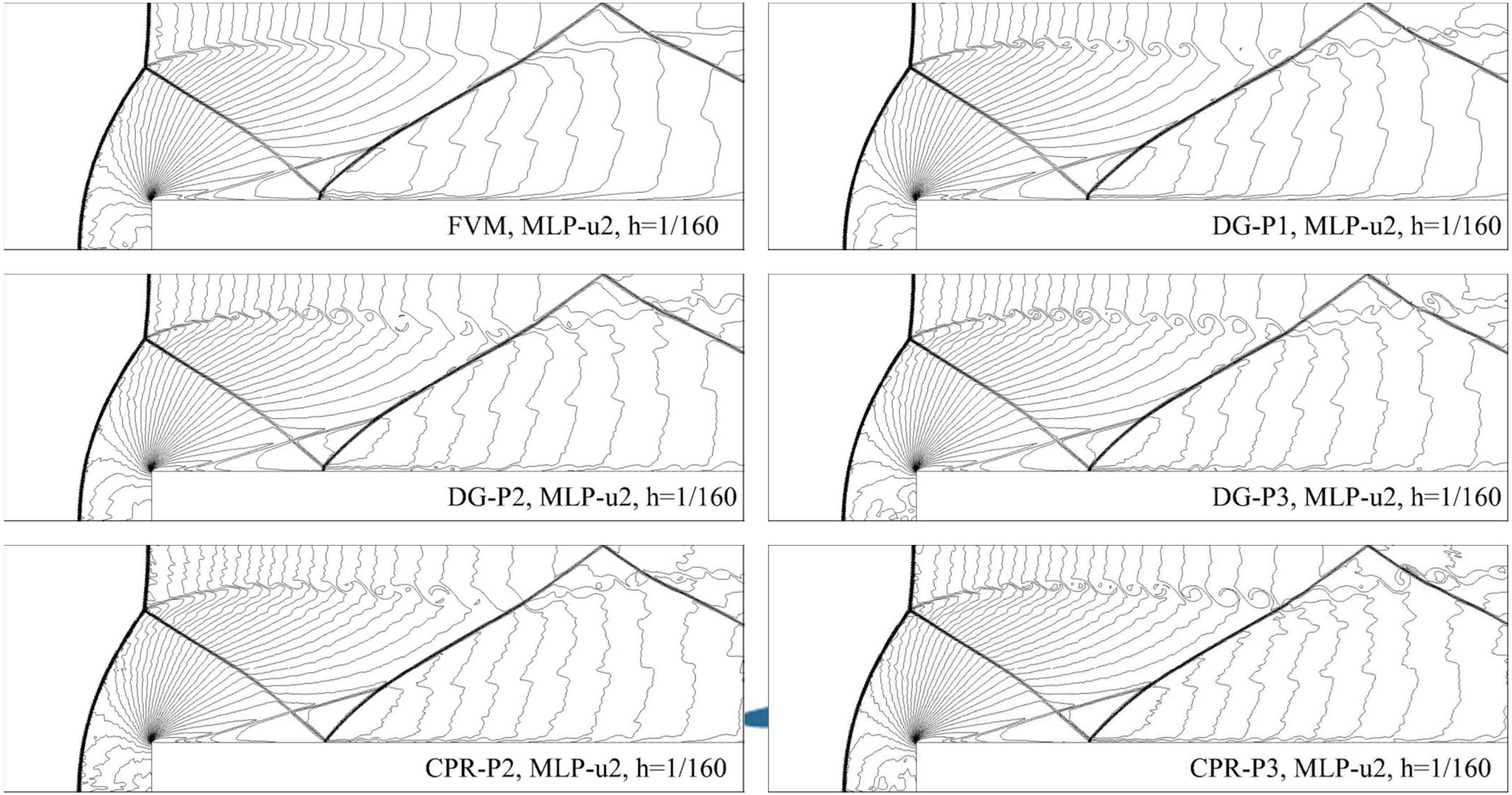

< Comparison of density contours >

Shock Interaction with Wedge

- **Schardin's Problem**
  - **Moving shock with $M_S = 1.34$ is passing the finite wedge**
  - **RoeM flux scheme with MLP-u slope limiters**
  - **Grid system: $h = 1/100$**

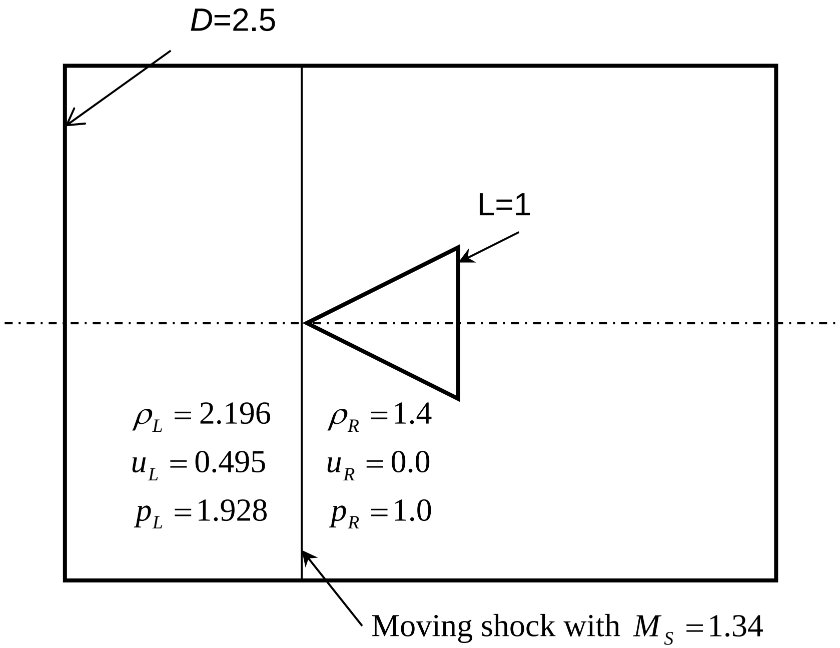

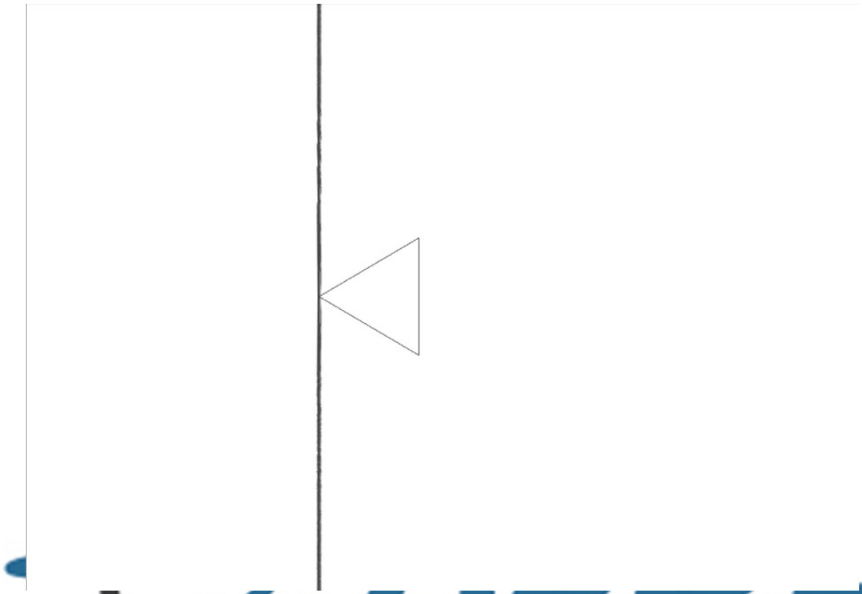

Shock Interaction with Wedge (Cont')

- **Higher-order MLP captures detailed flow structure.**

FVM, MLP-u1,h=1/100

DG-P1, MLP-u1,h=1/100

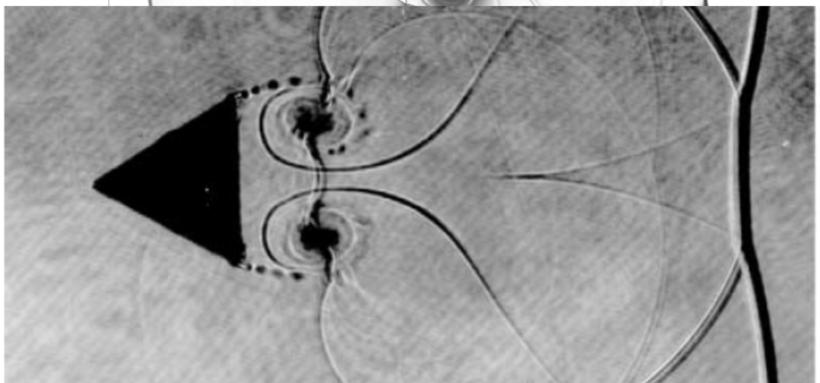

< Shadowgraphs, Chang & Chang, 2000 >

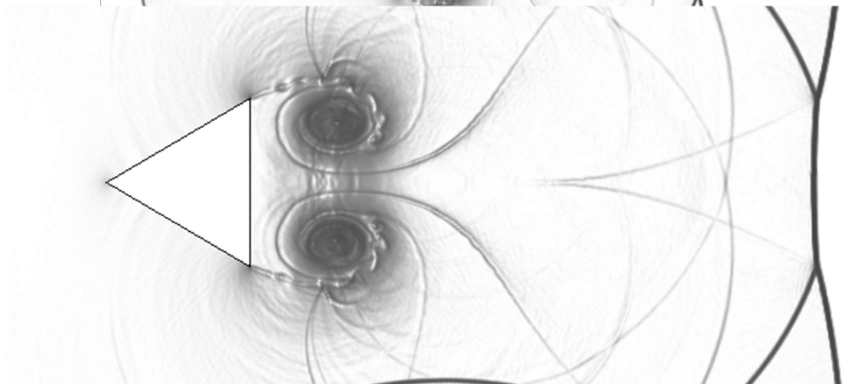

< Numerical Schlieren image, Present >

- **Computation & experiment: wedge angle = 60°, M_S = 1.34**

Shock Interaction with Wedge (Cont')

- **Long time calculation till *t = 4.78* (DG-P2-MLP)**

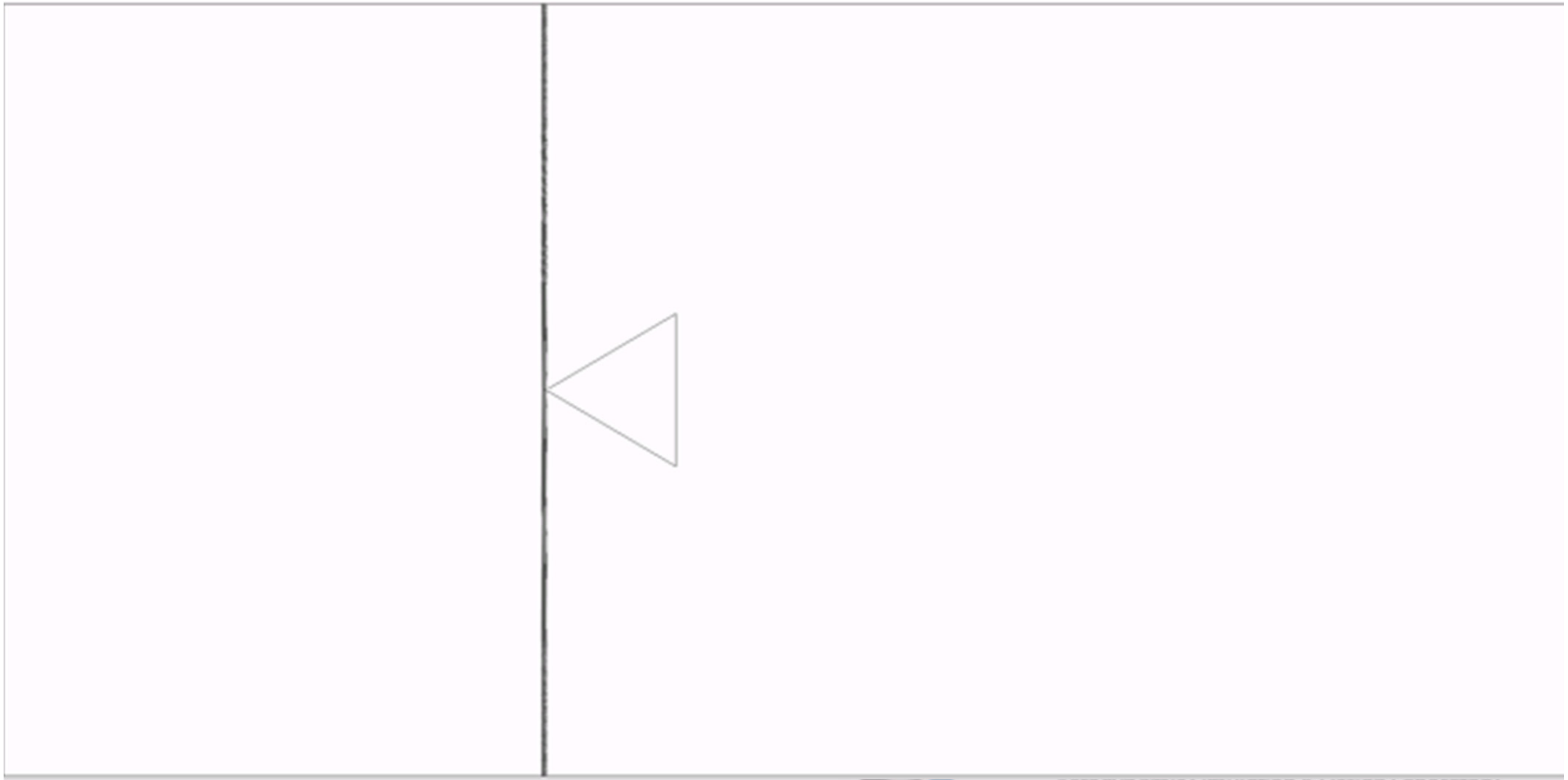

< Animation of long time evolution of shock-vortex shock >

Interaction of Shock Wave with Density Bubble

- **2-D Shock Wave with Circular Density Bubble**
  - **Moving shock with *Ms=3* impinging on density bubble (16.5% of the mean flow)**
  - **Kelvin-Helmholtz instability with complex vortex structure**
    - **Counterclockwise primary vortex surrounded by the tails of clockwise vortex**
  - **AUSMPW+ flux scheme with MLP-u slope limiters**
  - **Grid system: *h=L/100, L/200* (upper side only)**

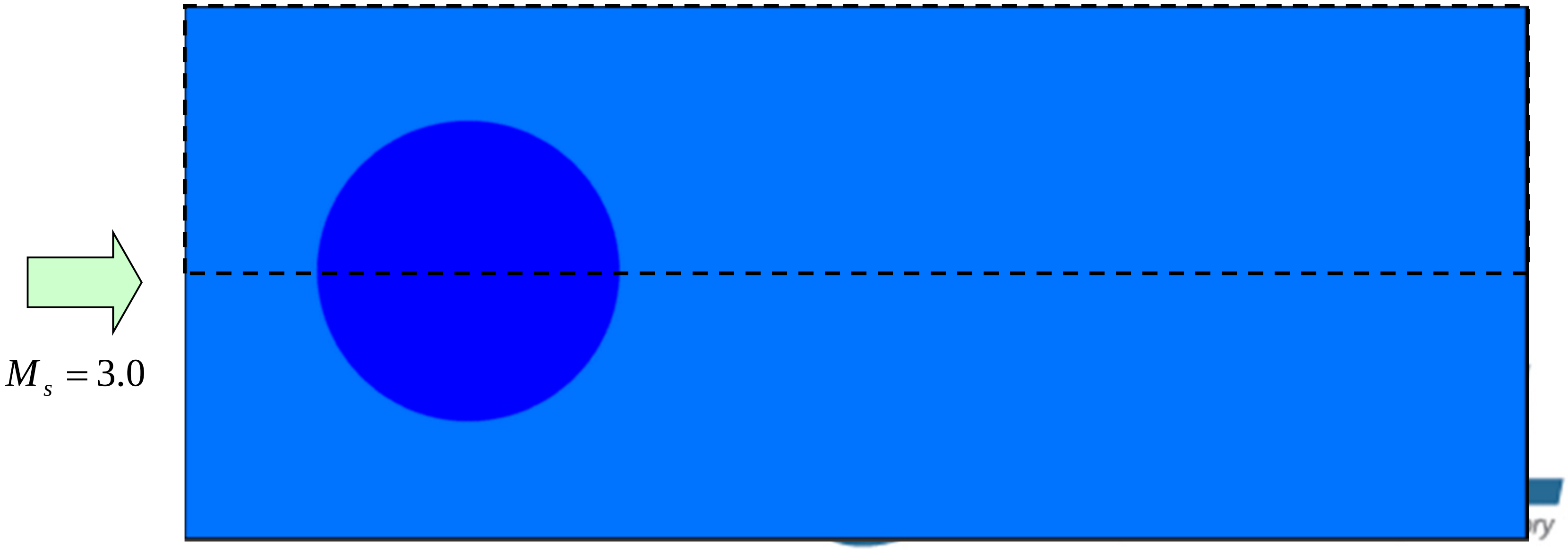

< Animation of density contour >

Interaction of Shock Wave with Density Bubble (Cont')

- **Medium grid** *(h=L/100)*

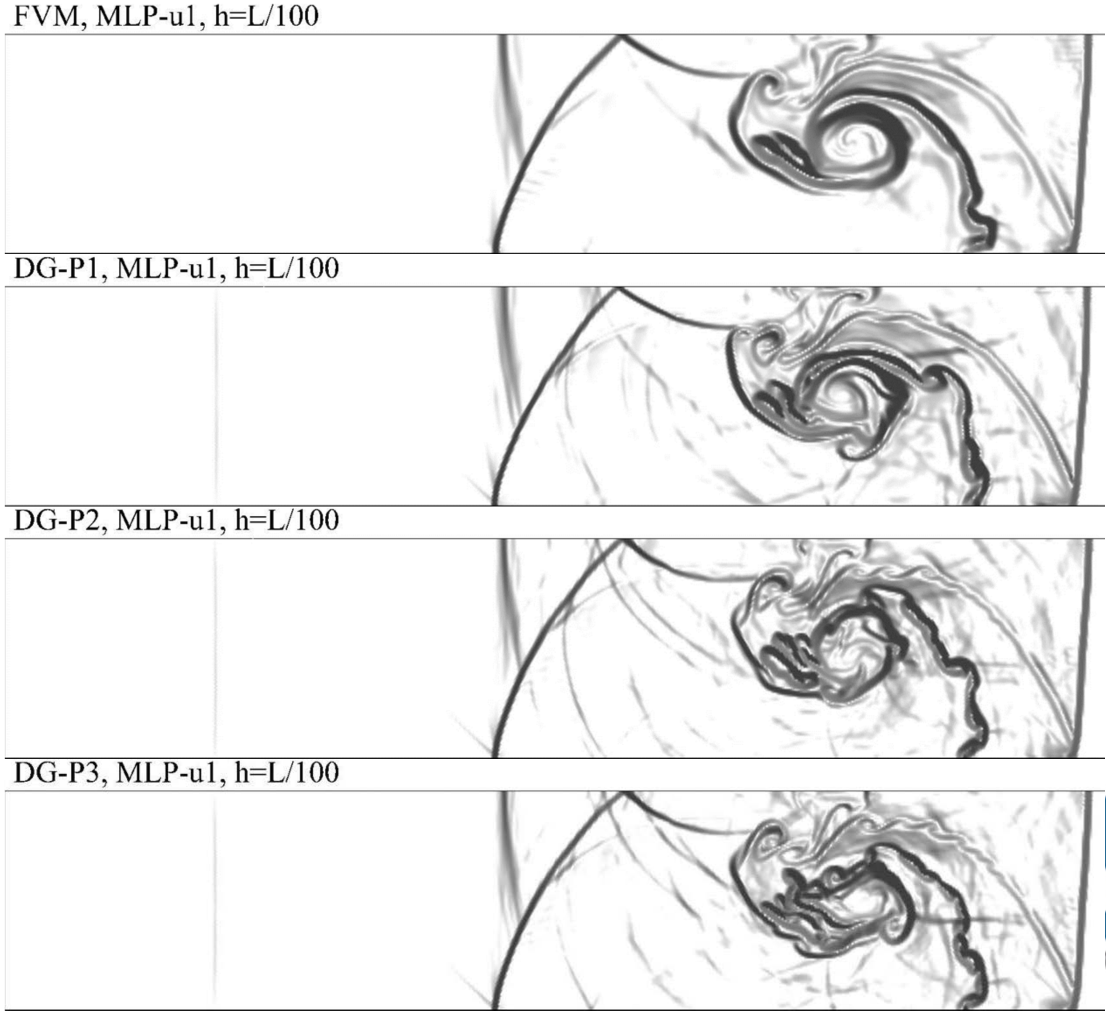

< Numerical Schlieren of density >

Interaction of Shock Wave with Density Bubble (Cont')

- **Fine grid** *(h=L/200)*

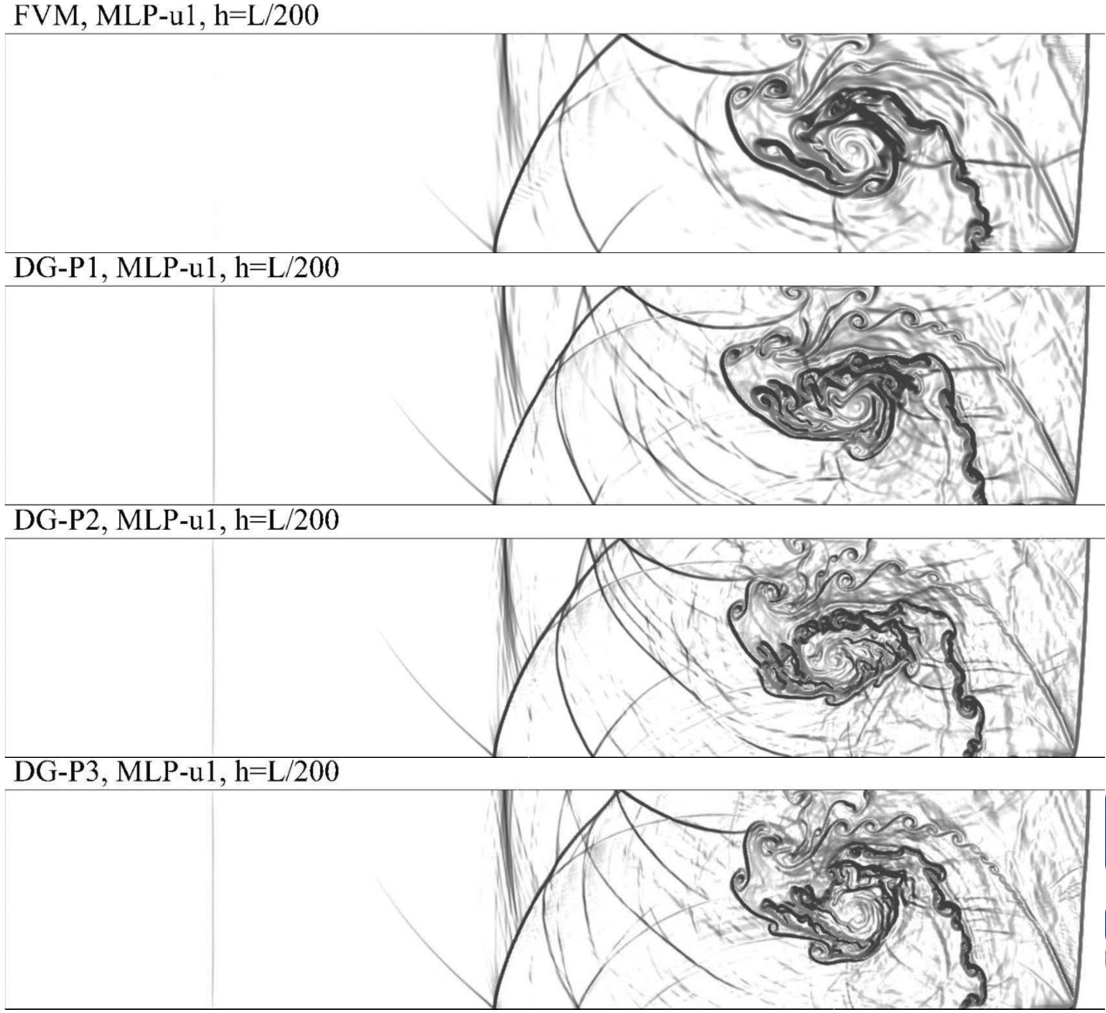

< Numerical Schlieren of density >

Interaction of Shock Wave with Density Bubble

- **3-D Shock Wave with Spherical Density Bubble**
  - **3-D extension of 2-D shock wave-density bubble interaction**
  - **Grid system with 8.9M tetrahedral elements**
    - Grid density is coarser than 2-D medium mesh.
  - **3-D baroclinic vortex structure**

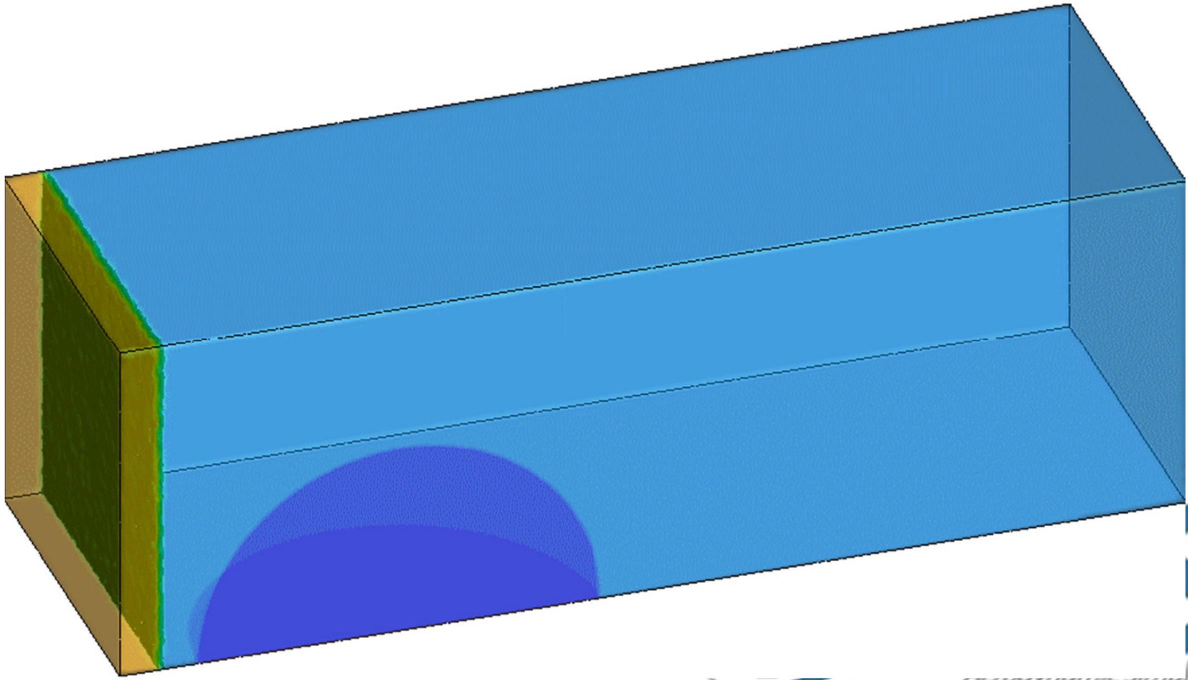

< Animation of density contour and iso-surface >

Interaction of Shock Wave with Density Bubble (Cont')

- **Torus-shaped vortex structure (*t = 3.5*)**

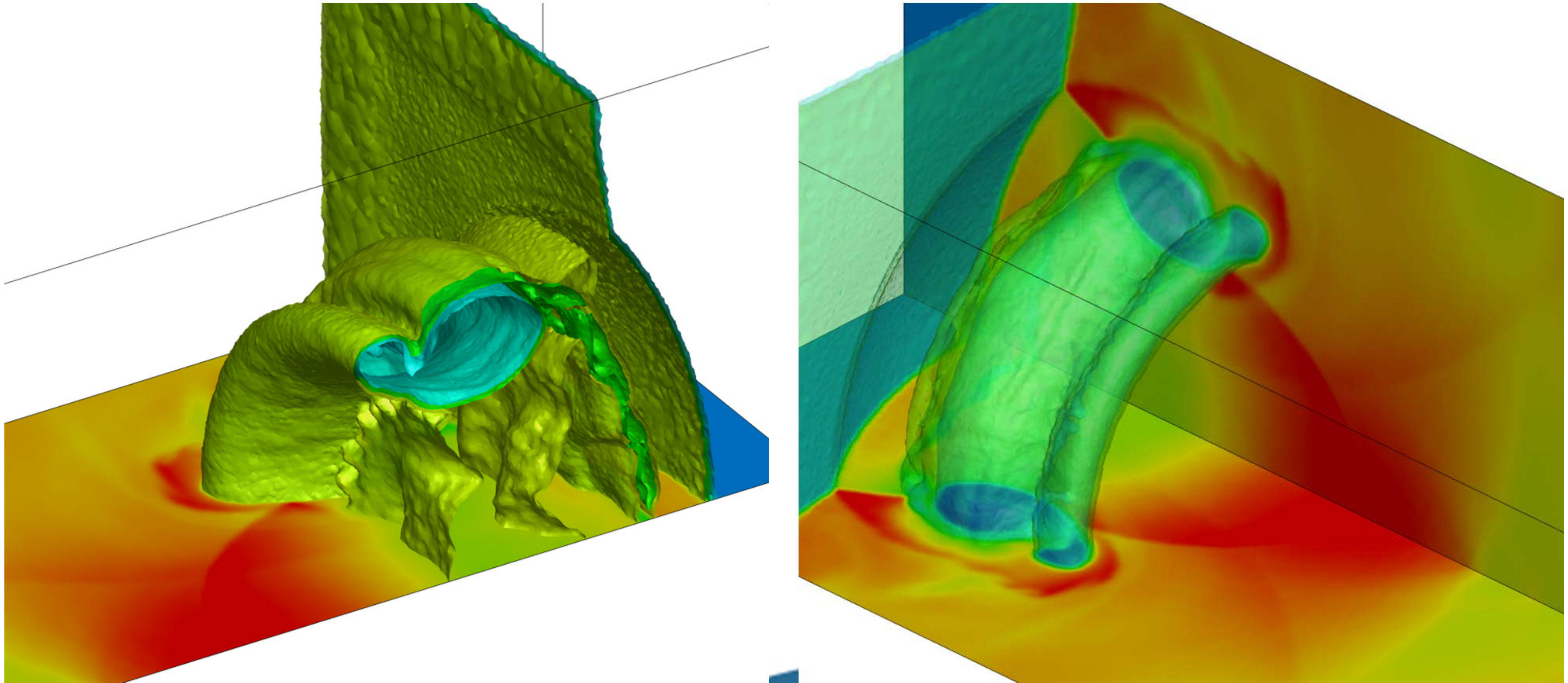

< Close-up view at t=3.5 >

Viscous Shock-Vortex Interaction

- **2-D Shock-Stong Vortex Interaction**
  - **Viscous interaction of weak shock (*$M_s = 1.2$*) with strong vortex *($Mv=1.0$)***

    $V_\theta = M_v r \exp\left(\left(1-r^2\right)/2\right)$ with $h=0.1$ on $[-10,30]\times[-10,30]$
  - **Multistage shock-vortex interaction**

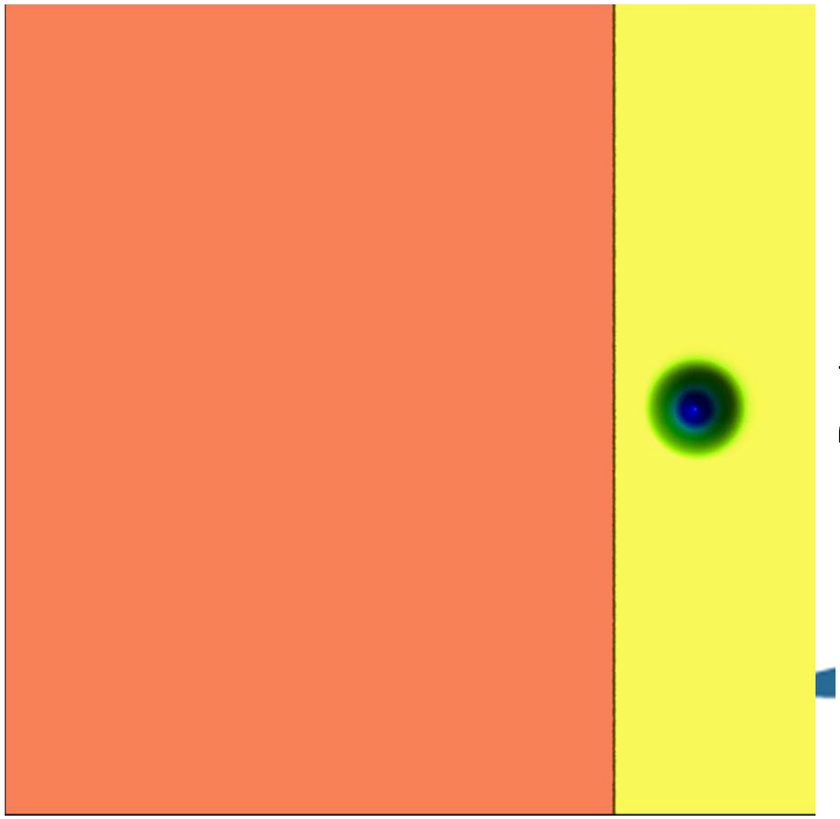

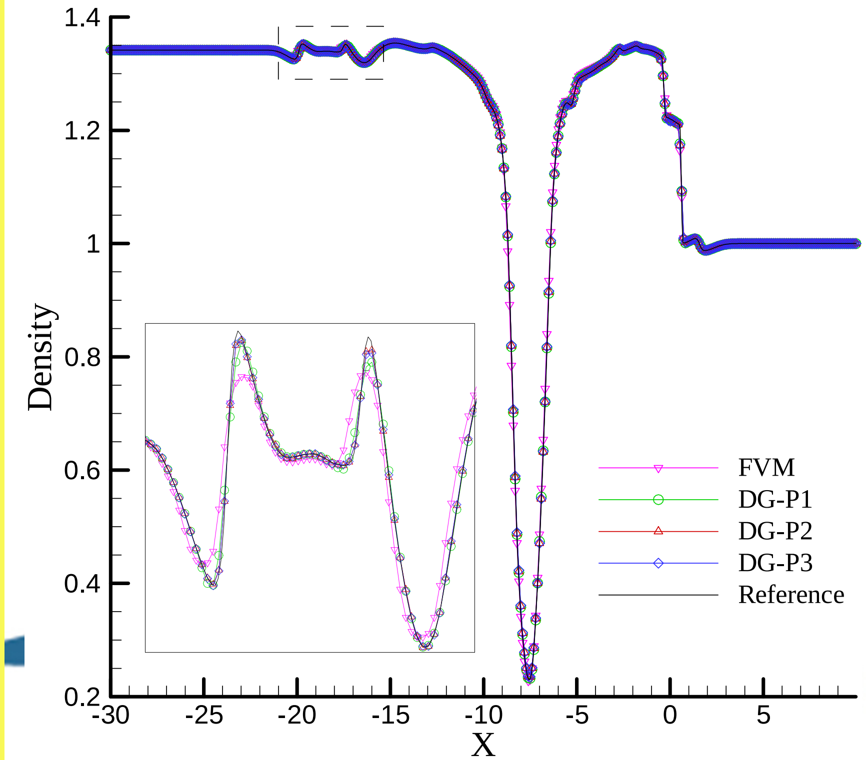

< Density distribution along center line t = 12 >

Oblique Shock-Mixing Layer Interactions

- **Oblique Shock-Compressible Mixing Layer Interaction (2-D Case)**
  - **Oblique shock** *(β=12°)* **impinging a spatially developing mixing layer**
    - Inflow perturbation

$$v' = \sum_{k=1}^{2} a_k \cos\left(2\pi k\, t/T + \phi_k\right)\exp\left(-y^2/b\right)$$

  - **By interacting downstream vortices and reflected shock, a series of shock and acoustic waves are developed.**
  - **RoeM flux scheme with MLP-u2 limiter**
  - **Grid system: uniform triangular grids on [40, 200] with *h = 0.75, 0.5*.**

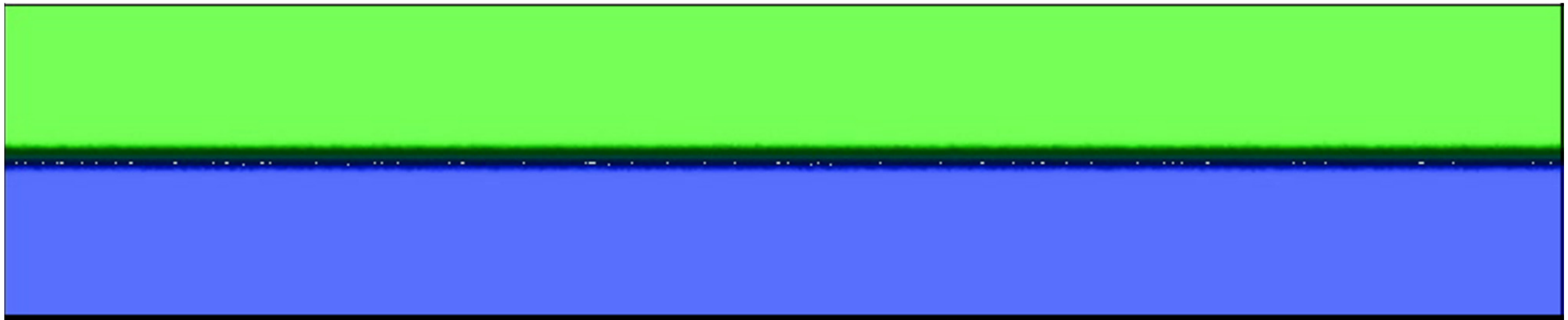

< Animation of numerical Schlieren >

Oblique Shock-Mixing Layer Interactions (Cont')

- **Coarse grid**

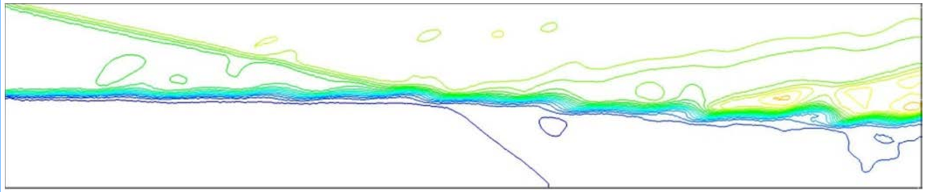

< Density, FVM-MLP >

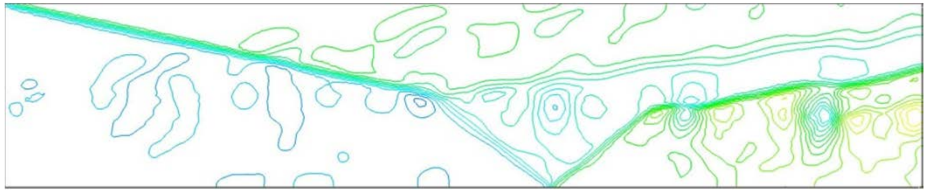

< Pressure, FVM-MLP >

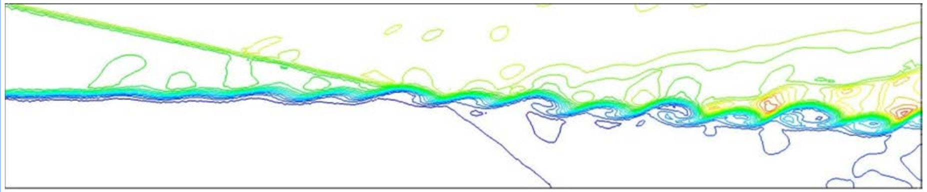

< Density, DG-P1-MLP >

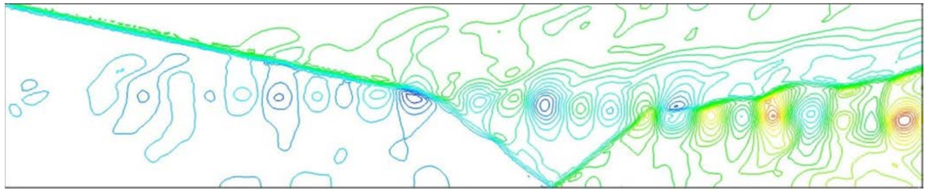

< Pressure, DG-P1-MLP >

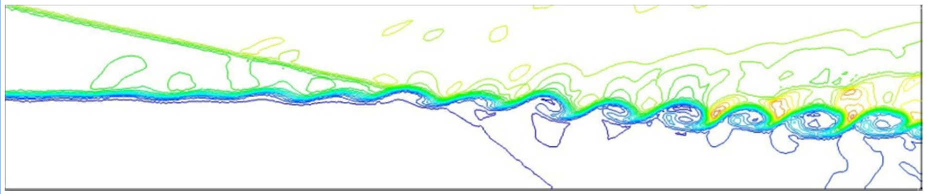

< Density, DG-P2-MLP >

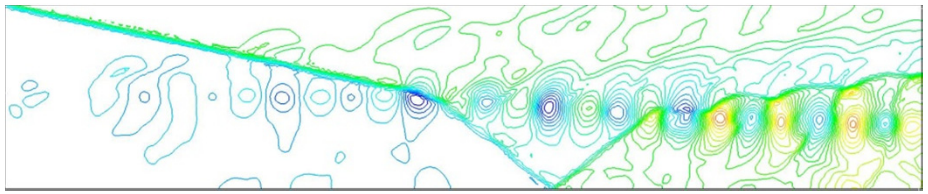

< Pressure, DG-P2-MLP >

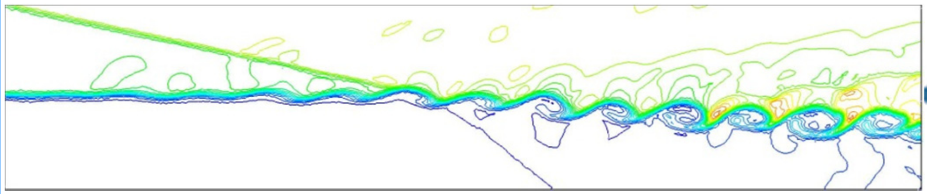

< Density, DG-P3-MLP >

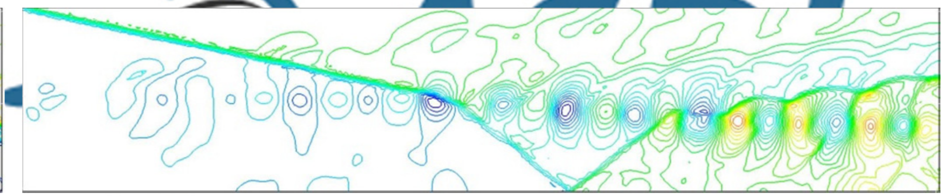

< Pressure, DG-P3-MLP >

Oblique Shock-Mixing Layer Interactions (Cont')

- **Medium grid**

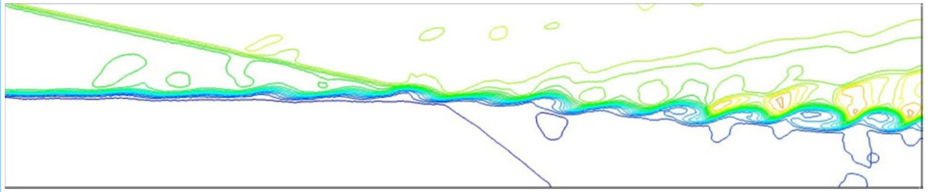

< Density, FVM-MLP >

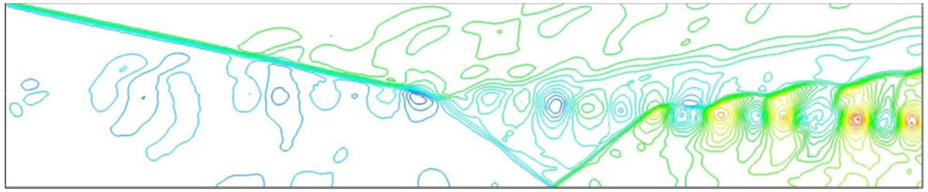

< Pressure, FVM-MLP >

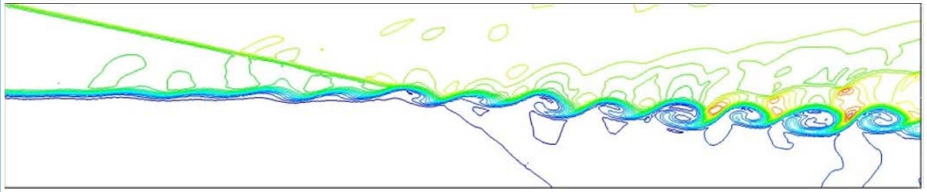

< Density, DG-P1-MLP >

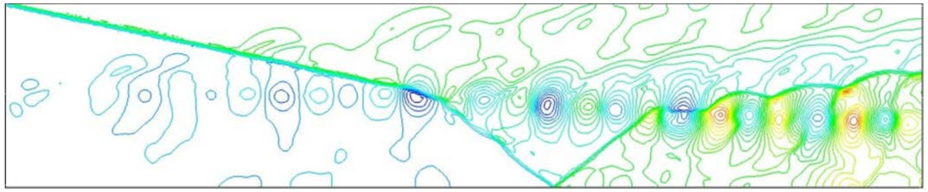

< Pressure, DG-P1-MLP >

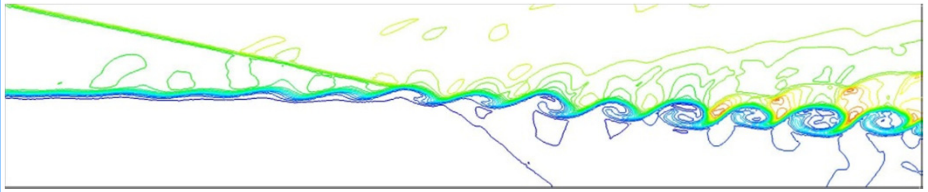

< Density, DG-P2-MLP >

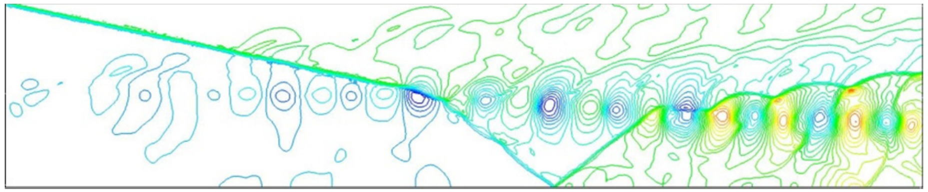

< Pressure, DG-P2-MLP >

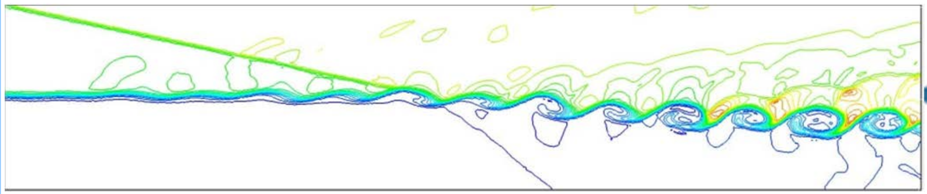

< Density, DG-P3-MLP >

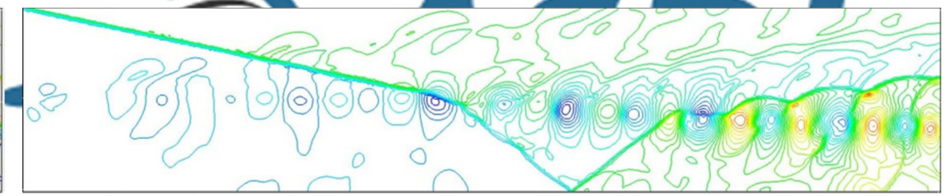

< Pressure, DG-P3-MLP >

Oblique Shock-Mixing Layer Interactions (Cont')

- **Oblique Shock-Compressible Mixing Layer Interaction (3-D Case)**
  - **Extending 2-D case into 3-D by adding spanwise perturbation**
    - Inflow perturbation

$$v' = \sum_{k=1}^{2} a_k \cos\left(2\pi k\, t/T + z/L_z + \phi_k\right) \exp\left(-y^2/b\right)$$

  - **Grid system with 7.8M tetrahedral elements**
    - Grid density is similar to 2-D medium mesh.

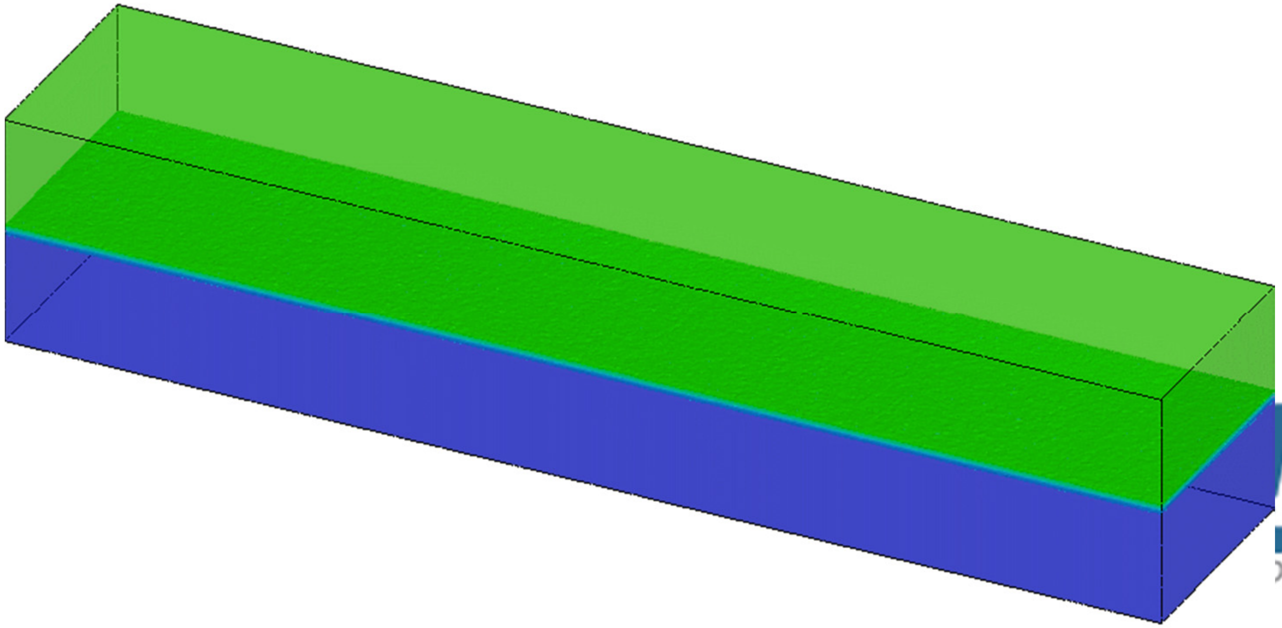

< Animation of density contour and iso-surface >

Oblique Shock-Mixing Layer Interactions (Cont’)

- **Sectional streamwise distribution**

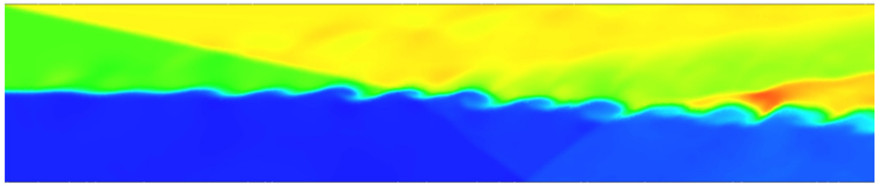

< Density, z = -15 >

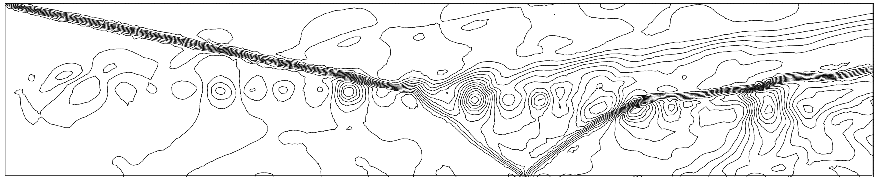

< Pressure, z = -15 >

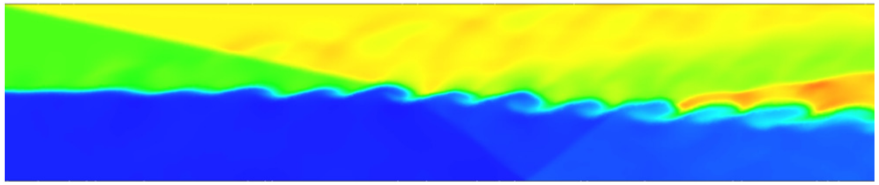

< Density, z = 0 >

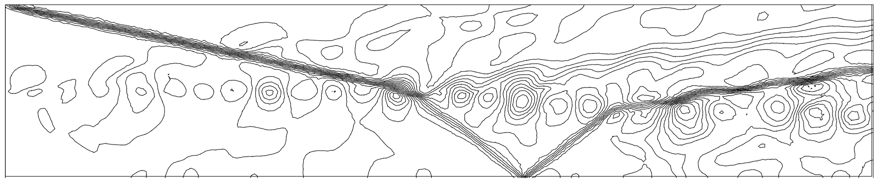

< Pressure, z = 0>

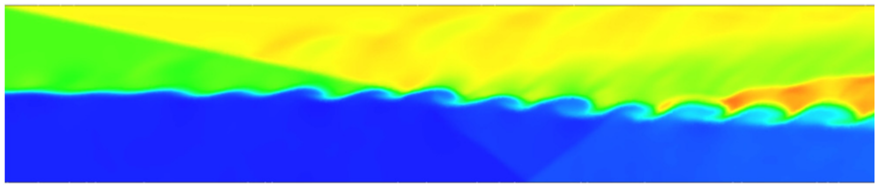

< Density, z = +15 >

< Pressure, z = +15 >

Conclusions

- **Hierarchical MLP limiting strategy for higher-order DG and CPR method to capture detailed flow structure of multi-dimensional flow physics**

- **MLP limiting strategy has been extended to arbitrary higher-order method.**
  - **Distinctive performances of MLP in FVM**
  - **Hierarchical MLP-based TC marker and MLP slope limiters**
    - The behavior of local smooth extrema combined with the augmented MLP condition

- **Characteristics of Hierarchical MLP Limiting**
  - **Without tuning parameter, the hierarchical MLP method maintains the accuracy in *continuous and discontinuous* flows.**
  - **MLP slope limiting is superior to (or at least competitive to) existing methods in terms of *accuracy and robustness*.**
  - ***Cost-effective* limiting without characteristic decomposition or complex limiting procedure**